Efficient Robust Model Predictive Control for Behaviorally Stable Vehicle Platoons

Peiyu Zhang, Daxin Tian, *Senior Member, IEEE,* Jianshan Zhou, Xuting Duan, Zhengguo Sheng, *Senior Member, IEEE,* Dezong Zhao, *Senior Member, IEEE,* Dongpu Cao, *Senior Member, IEEE* and Luzheng Bi, *Senior Member, IEEE*

***Abstract*—With increasing emphasis on vehicular automation and traffic efficiency, the management and coordination of platoon-based systems have become important. This research introduces a unique control framework based on a behavioral stability strategy, designed to enhance the cohesion of vehicle platoons and improve their ability to resist disturbances. Our approach integrates a vehicle scheduling system with a real-time platoon control mechanism to enhance the behavioral stability, robustness, and safety of the platoon. Given the heterogeneous nature of vehicles, we propose an optimal platoon formation model. This model strategically determines the number of platoons, arranges the sequence of vehicles within each platoon, and selects optimal cruising speeds to maximize platoon cohesion. To further enhance system robustness, a centralized robust model predictive controller is deployed for each platoon, ensuring stability against stochastic perturbations in vehicle dynamics and guaranteeing platoon safety. Finally, we conduct a simulation study involving multiple platoons with 20 heterogeneous vehicles to validate the effectiveness of the multi-layer optimization model.**

***Index Terms*—Connected and Automated Vehicles, Platoon Formation, Fuel Economy, Model Predictive Control, Robust Optimization.**

I. Introduction

VEHICULAR platooning depends on reliable communication technologies and advanced control methods to form clusters of vehicles traveling at a designated speed along the same route while maintaining safe inter-vehicle distances. Research by [1] and others indicates that approximately two-thirds of trucks in the United States are "platoon-capable". The benefits of vehicle platooning include enhancing road capacity [2]–[4], reducing pollutant emissions [5]–[7], and conserving energy [8]–[10]. Specifically, when the safe distance between two adjacent vehicles in a platoon is sufficiently close, the lead vehicle can reduce the air resistance on the surface of the following vehicle. Additionally, the cooperative nature between vehicles results in smoother control signals, further reducing fuel consumption. Literature [11] suggested that when the distance between two adjacent vehicles in a platoon is around 3.5 meters, the average fuel consumption of the entire platoon can be reduced by 9%.

A classic scenario of vehicular platooning typically refers to the formation of a convoy on a single lane [12]–[14]. The main challenges faced by single-lane platooning include the potential reduction in agility from an overly extended train-like formation, which may subsequently impact traffic flow. Furthermore, a fixed vehicular sequence and platoon speed might result in increased fuel consumption, thereby failing to enhance the environmental sustainability of the platoon. For instance, large-sized trucks have more aerodynamic drag, hence their position within a platoon plays a pivotal role in influencing the platoon's fuel consumption. Theoretical analyses and empirical studies conducted on cooperative vehicular platooning indicate that not all platoons are "inherently equal". The length of the platoon, its speed, and the sequence of vehicles can make one platoon configuration "greener" than another. Consistent with Literature [15], [16], given a set of vehicles, there may exist an "optimal green" platoon formation to achieve minimal fuel consumption. Additionally, [17] delved into the challenges of dynamically scheduling vehicles into platoons based on real-time traffic conditions and individual vehicular attributes. Their findings suggest that flexible scheduling, which factors in the real-time entry and exit of vehicles, can lead to more fluid and efficient traffic movements. Furthermore, [18] emphasized that different vehicle types, when sequenced optimally, can leverage the strengths of one to offset the limitations of another, creating a synergistic effect. [19] introduced bidirectional reference dynamics with proven string stability properties to mitigate the risk of string stability and cohesiveness loss in uncertain heterogeneous platoons. Therefore, it is necessary to provide insights into the formation composition of heterogeneous vehicles.

In addition to facilitating the formation of vehicle platoons, developing robust control mechanisms has become a critical area of research [20]. Although classical theories have made significant contributions to platoon control, several challenges

This research was supported in part by the National Key Research and Development Program of China under Grant No. 2022YFC3803700, in part by the National Natural Science Foundation of China under Grant No. U20A20155, Grant No. 52202391, Grant No. 62061130221 and Grant No. 62173012. *(Corresponding author: Daxin Tian.)*

Peiyu Zhang is with the School of Mechanical Engineering, Beijing Institute of Technology, Beijing 100081, China (e-mail: zpeiyu2@163.com).

Daxin Tian, Jianshan Zhou, Xuting Duan are with the Beijing Key Laboratory for Cooperative Vehicle Infrastructure Systems and Safety Control, Beijing Advanced Innovation Center for Big Data and Brain Computing, School of Transportation Science and Engineering, Beihang University, Beijing 100191, China (e-mail: dtian@buaa.edu.cn; jianshanzhou@foxmail.com; duanxuting@buaa.edu.cn).

Zhengguo Sheng is with the Department of Engineering and Design, University of Sussex, Richmond, Brighton BN1 9RH, U.K. (e-mail: z.sheng@sussex.ac.uk).

Dezong Zhao is with the James Watt School of Engineering, University of Glasgow, Glasgow G12 8QQ, U.K. (e-mail: dezong.zhao@glasgow.ac.uk).

Dongpu Cao is with the Department of Mechanical and Mechatronics Engineering, University of Waterloo, Waterloo, ON N2L 3G1, Canada (e-mail: dongpu.cao@uwaterloo.ca).

Luzheng Bi is with the School of Mechanical Engineering, Beijing Institute of Technology, Beijing 100081, China (e-mail: bhxblz@bit.edu.cn).

remain due to factors such as vehicle heterogeneity, vehicle-to-vehicle communication limitations, and uncertainties [20], [21]. Uncertainty, arising from various sources such as vehicle operations, sensor errors, and environmental conditions, presents a significant challenge to controller performance [21]. These stochastic perturbations can potentially breach safety boundaries, jeopardizing vehicle security. Therefore, designing robust platoon controllers for uncertain environments is essential to ensure both the formation and safe operation of platoons. The design of robust platoon controllers relies on forming cohesive multi-platoon structures characterized by high cohesion. Such cohesive formations create the necessary foundation for implementing effective control mechanisms. Once multiple platoons are established, introducing a centralized Robust Model Predictive Control (RMPC) method becomes essential to maintain coordination and ensure the safe operation of the platoons under uncertain conditions.

II. Literature Review

Early research on vehicular platooning was mainly based on optimal control theory, focusing on aspects like maintaining vehicles at desired speeds and safe distances [22]. Additionally, numerous researchers have been dedicated to exploring the fuel-saving effects of platoons under specific conditions, such as vehicle speed, separation distance, and vehicle sequence. An experiment was conducted by [23] on a platoon consisting of two distinct vehicle types. The test results demonstrated that, when the speed was set to 80 km/h with an inter-vehicle distance of 10m, the lead vehicle could achieve a 6% reduction in fuel consumption, while the trailing vehicle could realize a savings of 20% in fuel consumption (with distance ranging between 7m and 14m). Literature [1] further indicated that, in a scenario involving a platoon of three heavy trucks, the rear vehicle achieves minimum fuel consumption when the inter-vehicle distance exceeds 12 meters. The middle vehicle consumes the least fuel at relatively short distances, whereas the lead vehicle consistently incurs the highest fuel consumption irrespective of the set distance. These experiments underscore that vehicular platooning can enhance driving efficiency, concurrently fostering environmental sustainability.

Furthermore, the fuel efficiency of platooned vehicles is significantly influenced by the type of vehicle and its position within the platoon. According to [24], the benefits of fuel savings and emission reductions will be amplified in multi-platoon scenarios. Wind tunnel experiments by [11] and [25] indicated that larger vehicles experience greater aerodynamic drag than smaller cars. This difference becomes especially noticeable at higher speeds, as aerodynamic drag increases proportionally with the square of the velocity. According to tests in the literature [26], when a vehicle is located behind a large truck, the wind resistance of the behind vehicle is significantly reduced due to the large truck blocking the wind for the vehicle behind it. At this point, [15] presented an optimal platoon formation coupled with a fair benefit allocation mechanism (FAM) to ensure platoon stability. Their strategy delineates which vehicles should platoon and their respective speeds to optimize system benefits. [27] introduced a decentralized multi-agent system to address behavioral instability in platooning by redistributing benefits among members. [28] proposed an eco-friendly platoon formation strategy for a diverse fleet of electric vehicles on a single route. Utilizing a mathematical model-based optimization, they determined the optimal number and configuration of platoons to maximize energy savings and CO2 emission reduction. [29] investigated the influence of cooperative adaptive cruise control vehicle platooning on the capacity of multilane freeway merge bottlenecks, employing simulation experiments integrating car-following and lane-changing models with constraints on string length and inter-string time gaps. Inspired by the above research, we propose an optimal platoon formation method for multi-type vehicles, aiming to maximize the collective benefits (fuel economy) of the platoon.

From the perspective of platoon control, to counteract the uncertainties and disturbances inherent in vehicular platoon systems, numerous control methodologies have been proposed, such as sliding mode control [30], robust tube control [31], stochastic control [32], and robust model predictive control [33]. The main advantage of RMPC is its ability to efficiently regulate and manage the uncertainties and perturbations present in the system while taking into account future predictive models. It combines the advantages of traditional MPC with the robustness of robust control in order to provide a more reliable and flexible control solution. In addition, the RMPC method is able to adapt to changes in road conditions in real time, automatically responding to new information and recalculating the control strategy, thus ensuring the stability and safety of the vehicle platoon. [34] developed a novel approach to solve the RMPC problem for linear discrete-time systems with security constraints and objectives in the presence of bounded disturbances. [35] proposed a robust distributed model predictive platooning control for heterogeneous autonomous surface vehicles (ASVs) considering input constraints and external disturbances. Besides, they introduced an inter-vehicle safety constraint in the MPC optimization to prevent ASV collisions. [36] designed an RMPC algorithm to address the cooperative control of a connected vehicle platoon facing parameter uncertainty. By employing this RMPC algorithm, they derived a stability guarantee for the vehicle platoon system with model uncertainty. While methods of platoon formation and control have been explored in certain scenarios, there are few studies that comprehensively consider the integration of platoon formation with platoon control.

The objective of this paper is to introduce a comprehensive optimization framework designed to improve both the cohesion and robustness of vehicle platoons. Our approach begins with the strategic scheduling of vehicles, where each vehicle's data is transmitted to a centralized cloud-based controller. This centralized system plays a crucial role in determining the optimal configuration of vehicles within platoons, including both the ideal vehicle arrangement and the appropriate number of platoons needed. The primary focus during this scheduling phase is to maximize fuel efficiency and enhance the overall benefit of platooning by positioning vehicles in a way that optimizes aerodynamic advantages and improves the vehicle's

behavioral stability.

Once the optimal platoon formations have been established through this scheduling process, the focus shifts to ensuring the stability and safety of the platoons as they operate on the road. To achieve this, we introduce a centralized robust model of predictive controller for each distinct platoon. This RMPC model is specifically designed to address and mitigate the effects of uncertain disturbances, such as communication interferences, that could otherwise destabilize the platoon. By employing this robust control strategy, we aim to fortify the platoon system against uncertainties, ensuring that it can maintain its speed and spacing under varying uncertain disturbances. The key contributions of this paper are outlined as follows:

- We design a multi-layer optimization framework to improve fuel economy and robustness in multiple platoons. This sophisticated architecture integrates a fuel-efficient driving strategy, combining a comprehensive vehicle scheduling system with a real-time platoon control mechanism.
- We propose an optimal platoon formation model for heterogeneous vehicle types. The model determines the number of platoons, the sequence of vehicles within the platoon, and the platoon's optimal speed to enhance platoon cohesion and vehicle behavior stability.
- Based on the multi-formation system, we design a centralized RMPC controller for each individual platoon. This design not only addresses the uncertainties inherent in vehicular dynamics and external disturbances but also proactively manages potential disruptions in real-time scenarios.

The structure of this paper is organized as follows. Section III explains the motivation and basic assumptions of this paper. Section IV introduces the optimal platoon formation strategy, encompassing vehicle scheduling methods and an economic efficiency model. Section V presents the RMPC method under stochastic disturbances for a single platoon. Simulation results are provided and analyzed in Section VI, followed by simulation experiments detailed in Section VII. The work of this paper and future research work are concluded in Section VIII.

III. The Motivation and Basic Considerations

In the rapidly evolving field of automated transportation, vehicle platooning has emerged as a pivotal technology promising enhanced road capacity and reduced fuel consumption. Traditional vehicle formation control strategies, however, have not typically prioritized the specific order of vehicles within the platoon. Instead, these methods have been primarily concerned with maintaining a stable and safe distance between vehicles, without considering how the position of each vehicle could optimize overall team benefits, such as fuel efficiency or operational efficiency. According to literature [15] and [37], the increase in fuel efficiency primarily comes from platooning from the reduction in aerodynamic drag when vehicles travel closely together. However, this aerodynamic benefit is not evenly distributed among the different types of members. Vehicles in the middle of the platoon experience the most significant fuel savings, while the leading vehicle benefits the least. Consequently, it is necessary for decision-makers to re-optimize the vehicle sequence in platoons and then implement the control strategy.

Acknowledging this gap, this paper introduces a novel formation control model based on a behavioral stability strategy. Behavioral stability refers to the ability of a platoon to maintain its formation and cohesiveness over time, despite the inherent differences in benefits received by individual vehicles within the platoon. This concept is crucial because vehicles might have differing incentives to remain in the platoon due to unevenly distributed benefits such as fuel savings. Our model, by integrating behavioral stability, ensures that all vehicles in the platoon have sufficient incentive to remain part of the group. This maintains the overall structure and cohesion of the platoon, thus addressing a critical challenge in traditional platooning dynamics where individual vehicle benefits are not aligned with collective goals. Figure 1 shows the definition of behavioral stability and platoon cohesion.

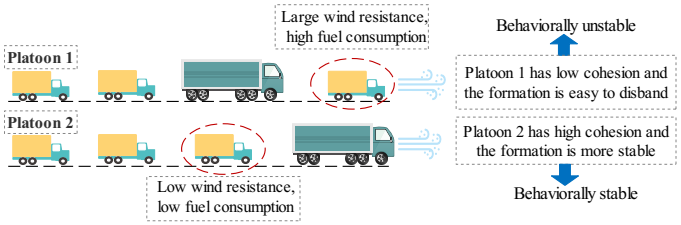

Fig. 1. Definition of behavioral stability and cohesion.

After establishing the vehicle dispatch and formation strategy to ensure behavioral stability within the platoon, our focus shifts to addressing the challenges posed by the uncertain disturbance. Specifically, we must consider the intercarrier interference that vehicles encounter during vehicle-to-vehicle communication while driving in formation. This interference, exacerbated by high doppler frequencies, can disrupt the critical communication signals between the leading vehicle and the following vehicles, which are essential for maintaining coordinated movement within the platoon. For each platoon, the leading vehicle is responsible for transmitting its acceleration data to the other vehicles through V2V communication [38], [39]. However, in conditions with high Doppler frequencies, these signals can become distorted, leading to significant intercarrier interference. Such disruptions seriously threaten communication integrity, which is vital for the platoon's synchronized operation. Traditional control methods often struggle to handle these interferences, making it difficult to maintain stable and safe platooning under these uncertain conditions [40], [41].

To address this critical issue, we propose a robust centralized model predictive control method specifically designed for vehicle formation control after the formation has been established. Following the initial multi-formation strategy, which handles the scheduling and positioning of vehicles, the focus shifts to controlling the platoon once it is formed. In this phase, the controller, located in the lead vehicle, oversees the entire

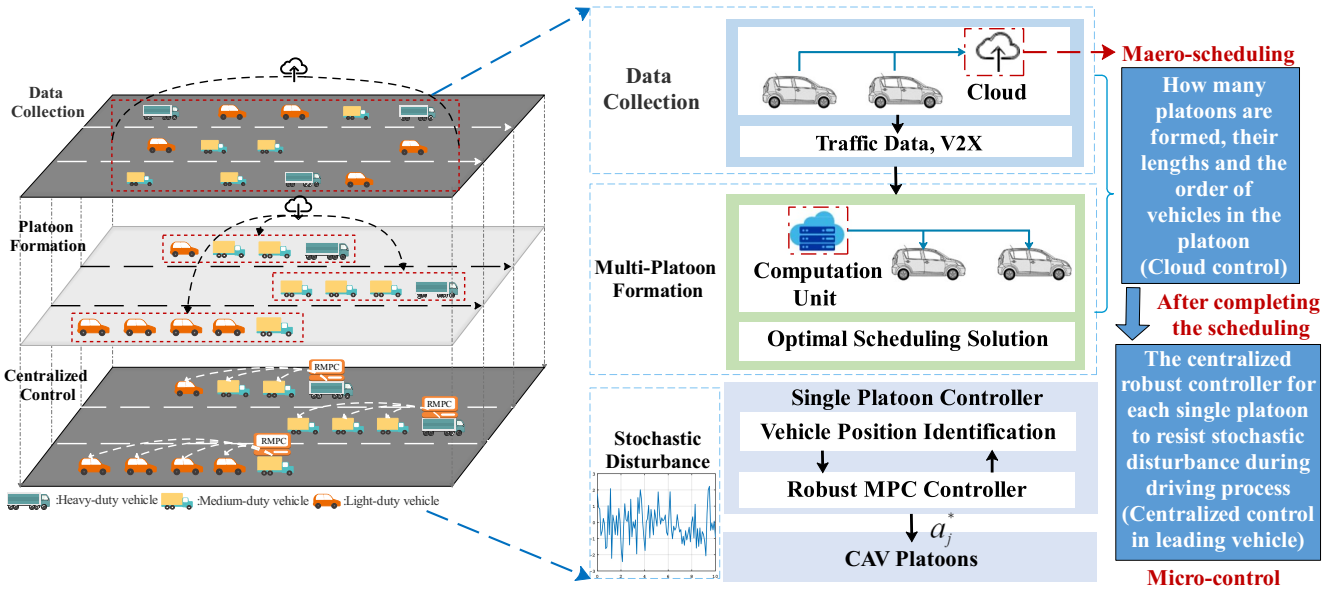

Fig. 2. The system scenario and architecture of this paper.

formation, ensuring that it can effectively deal with uncertain disturbances, such as intercarrier interference. By enhancing the robustness of the system, our approach aims to maintain the stability and safety of the platoon in real-world conditions where communication channels are often subject to various forms of interference. This research is driven by the necessity to ensure that vehicle platoons remain at fixed distances and speeds, even in uncertain dynamic environments. In summary, our research first addresses vehicle platoon formation at a macro level, ensuring behavioral stability by strategically assigning vehicles to optimize overall efficiency. Following this, we focus on robust control during platooning, tackling challenges like inter-carrier interference that can disrupt V2V communication. By combining strategic formation with robust control methods, we enhance the safety, stability, and efficiency of vehicle platoons in dynamic environments.

Our research is rooted in three fundamental hypotheses: 1. We hypothesize that highway systems commonly comprise more than two vehicle types; 2. We propose that a central cloud control center uniformly schedules the distribution behavior of vehicles at the macro level; 3. We posit that once platoon formations are established, the lead vehicle assumes the pivotal responsibility of coordinating and orchestrating fleet operations. Together, these hypotheses form the backdrop against which our research endeavors to develop a comprehensive framework for enhancing the efficiency and cohesion of multi-platoon formations on highways.

IV. Optimal Vehicle Platoon Formation Model

Figure 2 displays the system scenario and architecture of the multi-level optimization framework. In the first layer of our framework, we initiate the process of vehicle data collection, which forms the basis for subsequent decision-making and optimization tasks. By harnessing data from real-time traffic monitoring systems, we establish a comprehensive understanding of vehicle movements within the designated area, laying the groundwork for further analysis and optimization of platoon formation strategies. For the second layer of our framework, we address the complexity of traffic scenarios involving multiple vehicle types by introducing an ecologically based multi-platoon forming model. This model serves as the foundational component aimed at enhancing the cohesion of the formed platoon. Through this layer, we aim to optimize platoon formation strategies to enhance structural stability, ensuring that the resulting platoons exhibit high cohesion and maintain a tightly coordinated formation. The symbols in the model are as follows.

A. Notations in Model

Set:
$\mathcal{I} = \{1, \ldots, n\}$: Set of all vehicles, $i \in \mathcal{I}$;
$\mathcal{J} = \{1, \ldots, m\}$: Set of candidate platoon, $j \in \mathcal{J}$;
$\mathcal{K}_i$: A subset of platoons which are selected by vehicle i;
$\mathcal{M}_j$: A subset of all vehicles which belongs to platoon j.
Parameter:
k: The number of all candidate platoons;
v_i: The speed of vehicle i traveling alone, $i \in \mathcal{I}$;
β: The fuel consumption weight coefficient;
γ: The negative utility weight coefficient of vehicles;
F_i^0: The fuel consumption of vehicle i traveling alone;
C_i^0: The cost of vehicle i traveling alone;
U_i^j: The utility of vehicle i in platoon $j, j \in \mathcal{K}_i$;
$v_{\min}$: The minimum value of platoon speed;
$v_{\max}$: The maximum value of platoon speed;
G: A sufficiently large number.
Decision Variables:

$$y_j = \begin{cases} 1 & \text{If platoon } j \text{ is selected, } j \in \mathcal{J}; \\ 0 & \text{otherwise,} \end{cases}$$

$$x_{ji} = \begin{cases} 1 & \text{If vehicle } i \text{ is assigned to platoon } j, \ i \in \mathcal{I}; \\ 0 & \text{otherwise,} \end{cases}$$

v_j : The optimal speed of platoon j.

B. The Cost and Utility Function of Platoon Formation

According to the literature [42] and [43], the fuel consumption of vehicle i on the highway is related to the speed, so the following function is defined:

$$F_i^0(v) = \alpha_{i,1}^0 v^2 + \alpha_{i,2}^0 v + \alpha_{i,3}^0, \tag{1}$$

where $\alpha_{i,1}$, $\alpha_{i,2}$ and $\alpha_{i,3}$ are specific parameters for vehicle i. In this function, by reducing parameter $\alpha_{i,1}^0$, the air resistance can be reduced, which in turn saves energy. According to Comprehensive Modal Emission Model (CMEM) [42], $\alpha_{i,1}^0 = 0.5 A_i \Phi \rho$, where A_i is frontal area of vehicle i, Φ is air drag coefficient and ρ is a constant. $\alpha_{i,2}^0$ is the engine-related parameters and $\alpha_{i,3}^0$ stands for fuel consumption caused by acceleration and friction. Their values are derived from CMEM. Further, the travel cost of driving alone for vehicle i is:

$$C_i^0 = \beta F_i^0 (v_i), \tag{2}$$

where β is the fuel consumption weight coefficient. When vehicle i is located in platoon j, the air resistance function $\alpha_{ji,1}$ will become smaller, and the amount of reduction is related to the size n_j and sequence $\mathbf{S}_j$ of the platoon j. Experimental results from Literature [15] indicate that when the number of platoons exceeds 7, the overall platoon efficiency decreases. This suggests that more platoons do not necessarily lead to better performance. Thus, we define two sets $\mathcal{I}$ and $\mathcal{J}$. $\mathcal{I}$ contains all vehicles, $\mathcal{J}$ contains all candidate platoons and the number of all candidate platoons does not exceed $k = 5$. Assumed $\mathbf{S}_j$ is the sequence of vehicles in platoon $j \in \mathcal{J}$. The fuel consumption of vehicle i joint the platoon j:

$$F_i^j(v_j, n_j, \mathbf{S}_j) = \alpha_{ji,1}(n_j, \mathbf{S}_j) v_j^2 + \alpha_{ji,2} v_j + \alpha_{ji,3}, \tag{3}$$

where v_j is the speed of platoon j, n_j is the total number of vehicles in platoon j. Therefore, we define the cost function C_i^j of vehicle i when it belongs to platoon j:

$$C_i^j = \beta F_i^j (v_j, n_j, \mathbf{S}_j) + \gamma_i |v_j - v_i|. \tag{4}$$

The cost function C_i^j consists of two parts: the first part represents the travel cost by vehicle i to join platoon j. In contrast, the second part is a negative utility function with a weighting factor γ_i that describes the sensitivity of vehicle i to speed deviation. Specifically, when there is a deviation in the driving speed of platoon j from the expected speed of the vehicles, driving too fast will cause decision-makers to pay more attention to the safety of the platoon, resulting in an increase in negative utility; driving too slowly will result in additional delays and congestion.

By calculating the difference between Equation (2) and Equation (4), we define their difference as the utility or benefit of vehicle i joining the platoon j. The expression is:

$$\begin{aligned} &U_i^j (v_j, n_j, \mathbf{S}_j) = C_i^0 - C_i^j \\ &= \beta [F_i^0 (v_i) - F_i^j (v_j, n_j, \mathbf{S}_j)] - \gamma_i |v_j - v_i|, \end{aligned} \tag{5}$$

where C_i^0 is the travel cost of vehicle i when it is travelling alone, C_i^j is the travel cost when vehicle i belongs to platoon j. Here, we introduce binary decision variables y_j and x_{ji} to replace the optimal sequence $(n_j, \mathbf{S}_j)$. For instance, if $y_2 = 1$, then candidate platoon 2 is selected; if $x_{32} = 1$, vehicle 2 is assigned to platoon 3. Thus, the total utility of vehicles in platoon j has the following form:

$$\begin{aligned} &U_j (v_j, \mathbf{S}_j) = U_j (v_j, y_j, x_{ji}) = \sum_{i \in \mathcal{M}_j} U_i^j (v_j, y_j, x_{ji}) \\ &= \sum_{i \in \mathcal{I}} C_i^0 - \beta \sum_{i \in \mathcal{M}_j} F_i^j (v_j, y_j) - \sum_{i \in \mathcal{M}_j} \gamma_i |v_j - v_i| x_{ji}, \end{aligned} \tag{6}$$

where $\mathcal{M}_j$ is the set of vehicles belonging to platoon j. We will next introduce the optimal platoon formation model based on this utility function (6).

C. Optimal Platoon Formation

The utility of platoon j ($j \in \mathcal{K}_i$) is Equation (6), thus the all platoons utility can be deduced as:

$$\begin{aligned} &U (v_j, y_j, x_{ji}) = \sum_{i \in \mathcal{I}} C_i^0 - \sum_{j \in \mathcal{J}} \sum_{i \in \mathcal{M}_j} C_i^j = \sum_{i \in \mathcal{I}} \beta F_i^0 (v_i) \\ &- \sum_{j \in \mathcal{K}_i} \sum_{i \in \mathcal{M}_j} \beta F_i^j (v_j, y_j) - \sum_{j \in \mathcal{K}_i} \sum_{i \in \mathcal{M}_j} \gamma_i |v_j - v_i| x_{ji}, \end{aligned} \tag{7}$$

where

$$F_i^j(v_j, y_j) = [\alpha_{ji,1} v_j^2 + \alpha_{ji,2} v_j + \alpha_{ji,3}] y_j. \tag{8}$$

Furthermore, the optimal platoon formation model can be written as:

$$\max_{v_j, y_j, x_{ji}} U(v_j, y_j, x_{ji}) \tag{9a}$$

$$\text{s.t.} \sum_{j \in \mathcal{J}} y_j \leqslant k, \tag{9b}$$

$$v_j \leqslant G \cdot y_j,\ j \in \mathcal{J}, \tag{9c}$$

$$\sum_{i \in \mathcal{M}_j} x_{ji} = 1,\ j \in \mathcal{K}_i, \tag{9d}$$

$$z_{\min} \leqslant \sum_{i \in \mathcal{I}} x_{ji} \leqslant z_{\max},\ j \in \mathcal{K}_i, \tag{9e}$$

$$v_{\min} \leqslant v_j \leqslant v_{\max},\ j \in \mathcal{K}_i. \tag{9f}$$

The objective of function (9a) is to maximize the overall utility of all platoons. Constraint (9b) limits the total number of platoons formed to no more than k. Constraint (9c) specifies that only selected platoons can optimize their speed. Constraint (9d) ensures that each vehicle is assigned to only one open platoon. Additionally, constraint (9e) defines a range of the total number of vehicles in each open platoon row $i \in \mathcal{M}_j$. Finally, constraint (9f) sets bounds on the velocity of each forming platoon row. In our proposed multi-formation forming model, the decision variables play a pivotal role in determining the optimal configuration of platoons. These decision variables include the selection of the platoons y_j^*, the positioning of vehicles within the platoon x_{ji}^*, and the optimal speed of the platoon v_j^*. By strategically selecting the queue for each vehicle and assigning its position within the queue, the model optimizes the utilization of available space within the platoon, ensuring efficient and cohesive formations.

Building upon the foundational layer of the multi-platoon forming model (9), we next introduce a crucial component aimed at ensuring the safety and efficiency of each single-vehicle formation. Inspired by the principles outlined in the referenced literature and the cohesive decision-making facilitated by the multi-platoon forming model, we propose implementing a centralized robust control model for each formed single platoon. This centralized robust model predictive control concept will improve the robustness of the platoon in a highly dynamic and uncertain traffic environment, thereby further enhancing the safety and stability of the platoon system. Through the integration of this centralized robust control model, we aim to address uncertain disturbances inherent in real-world traffic environments, ensuring safety and efficient platooning operations.

V. Robust MPC model for single vehicle platoon

After successfully completing the vehicle scheduling and optimizing multiple formations to ensure behavioral stability, our focus now shifts to the control problem of a single formation. With the vehicles strategically positioned and the formation set, the next critical task is to manage the dynamic behavior of the formation as it maintains an optimal speed. A key challenge in this phase is addressing potential disturbances, such as those arising from V2V communication interference. High Doppler frequencies can disrupt these communication signals, leading to intercarrier interference, which makes it difficult for the vehicles in the convoy to maintain the necessary fixed spacing and speed, thereby increasing the risk of collisions.

Traditional control methods often struggle to cope with such interferences, contributing to an uncertain traffic environment. To tackle this issue, we have developed a centralized robust RMPC method specifically designed to enhance the platoon's resilience to intercarrier interference. By focusing on this specific type of disturbance and its impacts, our approach aims to ensure that the platoon operates safely and consistently, maintaining the desired spacing and speed even under uncertain conditions. This section delves into the strategies and methodologies employed to achieve this robust control, building on the foundational work of vehicle scheduling and formation optimization to ensure the reliable operation of vehicle platoons in dynamic environments.

A. Uncertain System State for Vehicle Platoons

For the vehicle i ($i \in \mathcal{M}_j$) in platoon j, the discrete dynamic system has the following form:

$$\begin{cases} p_i^j(t+1) = p_i^j(t) + \tau \cdot v_i^j(t) + \dfrac{\tau^2}{2} \cdot a_i^j(t); \\ v_i^j(t+1) = v_i^j(t) + \tau \cdot a_i^j(t), \end{cases} \tag{10}$$

where $p_i^j(t)$, $v_i^j(t)$ and $a_i^j(t)$ are the position, velocity, and acceleration (control signal) of the vehicle i in platoon j. Besides, τ is a relatively small time interval of continuous time, r is a constant representing the reaction time and L is the vehicle length. According to literature [44], the spacing error and velocity error of the platoon j are defined as:

$$\begin{cases} \triangle\, e_{p,i}^j(t) = p_{i-1}^j(t) - p_i^j(t) - r \cdot v_i^j(t) - L; \\ \triangle\, e_{v,i}^j(t) = v_{i-1}^j(t) - v_i^j(t). \end{cases} \tag{11}$$

Thus, we can deduce the state error of the platooning vehicle

$$\begin{aligned} \begin{bmatrix} \triangle e_{p,i}^j(t+1) \\ \triangle e_{v,i}^j(t+1) \end{bmatrix} = \begin{bmatrix} 1 & \tau \\ 0 & 1 \end{bmatrix} \begin{bmatrix} \triangle e_{p,i}^j(t) \\ \triangle e_{v,i}^j(t) \end{bmatrix} + \begin{bmatrix} \frac{\tau^2}{2} \\ \tau \end{bmatrix} a_{i-1}^j(t) \\ + \begin{bmatrix} -(\frac{\tau^2}{2} + r\tau) \\ -\tau \end{bmatrix} a_i^j(t). \end{aligned} \tag{12}$$

The system state is defined as $\boldsymbol{e}_i^j(t) = [\triangle e_{p,i}^j(t), \triangle e_{v,i}^j(t)]^{\mathrm{T}}$, and the dynamics system can be represented as follows:

$$\boldsymbol{e}_i^j(t+1) = \boldsymbol{A}\boldsymbol{e}_i^j(t) + \boldsymbol{B}a_i^j(k) + \boldsymbol{D}a_{i-1}^j(k), \tag{13}$$

where $\boldsymbol{A} = \begin{bmatrix} 1 & \tau \\ 0 & 1 \end{bmatrix}$, $\boldsymbol{B} = \begin{bmatrix} -(\frac{\tau^2}{2} + r\tau) \\ -\tau \end{bmatrix}$, $\boldsymbol{D} = \begin{bmatrix} \frac{\tau^2}{2} \\ \tau \end{bmatrix}$. Furthermore, in order to obtain a compact form of systematic error about platoon j. We define the following variables:

$$\begin{aligned} \boldsymbol{e}_j(t) &= \mathrm{col}\{\boldsymbol{e}_1^j(t), \boldsymbol{e}_2^j(t), \ldots, \boldsymbol{e}_i^j(t), \ldots\}, i \in \mathcal{M}_j, \\ \boldsymbol{a}_j(t) &= \mathrm{col}\{a_1^j(t), a_2^j(t), \ldots, a_i^j(t), \ldots\}, i \in \mathcal{M}_j. \end{aligned} \tag{14}$$

The compact form of platoon j has the following form:

$$\boldsymbol{e}_j(t+1) = \boldsymbol{G}_A\boldsymbol{e}_j(t) + \boldsymbol{G}_B\boldsymbol{a}_j(t) + \boldsymbol{G}_D a_{j,0}(t), \tag{15}$$

where $a_{j,0}(t)$ is the acceleration of leading vehicle in platoon j, and matrices $\boldsymbol{G}_A$, $\boldsymbol{G}_D$ and $\boldsymbol{G}_B$ are defined by:

$$\boldsymbol{G}_A = \mathrm{diag}\left\{\boldsymbol{A}, \boldsymbol{A}, \ldots, \boldsymbol{A}\right\}, \boldsymbol{G}_D = \mathrm{col}\{\boldsymbol{D}, \boldsymbol{0}, \boldsymbol{0}, \ldots, \boldsymbol{0}\},$$

$$\boldsymbol{G}_B = \begin{bmatrix} \boldsymbol{D} & \boldsymbol{0} & \boldsymbol{0} & \cdots & \boldsymbol{0} & \boldsymbol{0} \\ \boldsymbol{B} & \boldsymbol{D} & \boldsymbol{0} & \cdots & \boldsymbol{0} & \boldsymbol{0} \\ \boldsymbol{0} & \boldsymbol{B} & \boldsymbol{D} & \cdots & \boldsymbol{0} & \boldsymbol{0} \\ \vdots & \vdots & \vdots & \cdots & \vdots & \vdots \\ \boldsymbol{0} & \boldsymbol{0} & \boldsymbol{0} & \cdots & \boldsymbol{B} & \boldsymbol{D} \end{bmatrix}.$$

Remark 1: In general, the leading vehicle in a platoon provides a reference trajectory for the following vehicles, allowing for the acceleration $a_{j,0}(t)$ of the lead vehicle to be determined in advance. According to literature [45], we assume that the leading vehicle is driving at an optimal speed v_j, based on ecological driving obtained by the planning layer. Therefore, the reference acceleration $a_{j,0}(t)$ of the leading vehicle is set to $0\,m/s^2$ as the equilibrium state of the vehicle motion. Therefore, (15) can be written as:

$$\boldsymbol{e}_j(t+1) = \boldsymbol{G}_A\boldsymbol{e}_j(t) + \boldsymbol{G}_B\boldsymbol{a}_j(t). \tag{16}$$

In real-world scenarios, the robustness of controllers cannot be guaranteed due to the discrepancy between traditional control models and discretized vehicle dynamics systems. For instance, in low-visibility environments, sensors may be influenced by external factors such as rain or snow, resulting in inaccurate measurement information and model mismatch between the control model and the actual vehicle being controlled. Therefore, we consider a more realistic model that

incorporates comprehensive uncertainty caused by measurement errors, uncertain traffic conditions, and model mismatch. Thus, the uncertain dynamic system of platoon j is:

$$\boldsymbol{e}_j(t+1) = \boldsymbol{G}_A \boldsymbol{e}_j(t) + \boldsymbol{G}_B \boldsymbol{a}_j(t) + \boldsymbol{G}_w \boldsymbol{w}_j(t), \tag{17}$$

where $\boldsymbol{w}_j(t)$ is a lumped uncertainty and $\boldsymbol{G}_w$ is a known matrix which is related to uncertain perturbation $\boldsymbol{w}_j(t)$. In this paper, we assume that the uncertain disturbance belongs to a Ball uncertain set: $\boldsymbol{w}_j(t) \in \text{Ball}_\Phi$, and the Ball uncertain set has the form:

$$\text{Ball}_\Phi = \{\|w_j^i(t)\|_2 \leq \Phi, i \in \mathcal{M}_j\}. \tag{18}$$

Remark 2: For $p \in [1, \infty]$, we define the p-norms $\|\cdot\|_p$ on $\mathbb{C}^n$ and $\mathbb{R}^n$ by the relation

$$\|x\|_p = \begin{cases} \left(\sum_i |x_i|^p\right)^{1/p}, & 1 \leq p < \infty, \\ \lim_{p\to\infty} \|x\|_p = \max_i |x_i|, & p = \infty. \end{cases} \tag{19}$$

The 2-norm of uncertain perturbation in Ball_Φ uncertain set is: $\sqrt{|\boldsymbol{w}_j(t)|^2} \leq \Phi$. Unlike bounded disturbances (robust min-max), Ball uncertain set is a new construction form for uncertain disturbances, which can improve the robustness of the control system and prevent it from being too conservative.

In addition, in order to ensure the safety of vehicle movement, we propose the following related constraints for vehicle i in platoon j:

$$\begin{cases} e_{p,i}^{\min} \leq \triangle e_{p,i}^j(t) - D \leq e_{p,i}^{\max}; & (20) \\ e_{v,i}^{\min} \leq \triangle e_{v,i}^j(t) \leq e_{v,i}^{\max}; & (21) \\ a_i^{\min} \leq a_i^j(t) \leq a_i^{\max}. & (22) \end{cases}$$

The constraints related to position and speed error are represented by equations (20) and (21) in the above formula, respectively. Specifically, D is the desired vehicle distance, the $e_{p,i}^{\min}$ and $e_{p,i}^{\max}$ denote the upper and lower bounds of the position error of the workshop, while $e_{v,i}^{\min}$ and $e_{v,i}^{\max}$ represent the upper and lower bounds of the speed error of the workshop. Equation (22) specifies the upper and lower bounds related to vehicle acceleration, while $a_i^{\min}$ and $a_i^{\min}$ denote the upper and lower bounds of the acceleration of vehicle i. These constraints ensure that the position and speed errors remain within the prescribed bounds and the vehicle acceleration is limited to a safe range during the control process. The proper enforcement of these constraints is crucial for ensuring the safe and effective operation of the system.

Next, we construct the system constraint set for platoon j. At time t, we suppose that $\boldsymbol{e}_j^{\min} = \text{col}\left\{e_{p,i}^{\min}, e_{v,i}^{\min}, i \in \mathcal{M}_j\right\}$, $\boldsymbol{e}_j^{\max} = \text{col}\left\{e_{p,i}^{\max}, e_{v,i}^{\max}, i \in \mathcal{M}_j\right\}$, thus the lower and upper bounds of system state $\boldsymbol{e}_j(t)$ is: $\boldsymbol{e}_j^{\min} \leq \boldsymbol{e}_j(t) \leq \boldsymbol{e}_j^{\max}$. Similarly, let $\boldsymbol{a}_j^{\min} = \text{col}\left\{a_i^{\min}, i \in \mathcal{M}_j\right\}$ and $\boldsymbol{a}_j^{\max} = \text{col}\left\{a_i^{\max}, i \in \mathcal{M}_j\right\}$, the bounds of acceleration about total vehicles are: $\boldsymbol{a}_j^{\min} \leq \boldsymbol{a}_j(t) \leq \boldsymbol{a}_j^{\max}$. Then, the platoon system constraint set at time t can be summarized as

$$\begin{cases} \mathcal{E} = \left\{\boldsymbol{e} : \boldsymbol{e}_j^{\min} \leq \boldsymbol{e}_j(t) \leq \boldsymbol{e}_j^{\max}\right\}; \\ \mathcal{A} = \left\{\boldsymbol{a} : \boldsymbol{a}_j^{\min} \leq \boldsymbol{a}_j(t) \leq \boldsymbol{a}_j^{\max}\right\}. \end{cases} \tag{23}$$

B. Closed-loop Robust MPC Formulation for Vehicle Platoon

In this paper, we employ a linear feedback control strategy to achieve closed-loop control. The specific form of this control strategy is:

$$\boldsymbol{a}_j(t) = \boldsymbol{k}_j \boldsymbol{e}_j(t) + \boldsymbol{u}_j(t), \tag{24}$$

where $\boldsymbol{k}_j$ can obtained off-line and $\boldsymbol{u}_j(t)$ is a new decision variable. Thus, the closed-loop form of the state equation is:

$$\begin{aligned} \boldsymbol{e}_j(t+1) &= \boldsymbol{G}_A \boldsymbol{e}_j(t) + \boldsymbol{G}_B \boldsymbol{a}_j(t) + \boldsymbol{G}_w \boldsymbol{w}_j(t) \\ &= \boldsymbol{G}_A \boldsymbol{e}_j(t) + \boldsymbol{G}_B[\boldsymbol{k}_j \boldsymbol{e}_j(t) + \boldsymbol{u}_j(t)] + \boldsymbol{G}_w \boldsymbol{w}_j(t) \\ &= \boldsymbol{G}_\psi \boldsymbol{e}_j(t) + \boldsymbol{G}_B \boldsymbol{u}_j(t) + \boldsymbol{G}_w \boldsymbol{w}_j(t), \end{aligned} \tag{25}$$

where $\boldsymbol{G}_\psi = \boldsymbol{G}_A + \boldsymbol{G}_B \boldsymbol{k}_j$. The goal of each platoon system is to achieve a stable platoon control with fixed inter-vehicle distances, while simultaneously reducing the influence of uncertain disturbances during driving and outputting real-time control signals for the vehicles. Based on the worst-case principle [46], we construct an MPC-based centralized robust control model for each formed platoon. Specifically, let N_p is the prediction time domain, $\boldsymbol{e}_j(t+h|t)$ and $\boldsymbol{u}_j(t+h|t)$ are the predicted state and predicted acceleration, $\boldsymbol{w}_j(t+h|t)$, where $h = 1, ..., N_p$. In addition, the vehicle state error $\boldsymbol{e}(t|t)$ at the initial time t is known. Thus, the objective function of platoon system j at time t is:

$$\mathcal{L}(t) = \sum_{h=0}^{N_p-1} \mathcal{L}_p(\boldsymbol{e}_j(t+h|t), \boldsymbol{u}_j(t+h|t)) + \Psi(\boldsymbol{e}_j(t+N_p|t)), \tag{26}$$

where $\mathcal{L}_p(\cdot)$ is stage objective function and $\Psi(\cdot)$ is terminal objective function. Their specific expressions are:

$$\begin{aligned} &\mathcal{L}_p(\cdot) = \boldsymbol{e}_j(t+h|t)^{\mathrm{T}} \boldsymbol{Q}\, \boldsymbol{e}_j(t+h|t) + \boldsymbol{u}_j(t+h|t)^{\mathrm{T}} \boldsymbol{R}\, \boldsymbol{u}_j(t+h|t), \\ &\Psi(\cdot) = \boldsymbol{e}_j(t+N_p|t)^{\mathrm{T}} \boldsymbol{Q}_N\, \boldsymbol{e}_j(t+N_p|t), \end{aligned} \tag{27}$$

where $\boldsymbol{Q}$, $\boldsymbol{R}$ and $\boldsymbol{Q}_N$ are positive definite diagonal matrices of known dimensions. For notational simplicity, we introduce compact forms of the error state, control, and uncertain perturbations of the platoon system in all predicted time slots:

$$\begin{cases} \boldsymbol{X}_j = \text{col}\{\boldsymbol{e}_j(t+h|t), h = 1, 2, \ldots, N_p\}; \\ \boldsymbol{U}_j = \text{col}\{\boldsymbol{u}_j(t+h|t), h = 0, 1, \ldots, N_p - 1\}; \\ \boldsymbol{W}_j = \text{col}\{\boldsymbol{w}_j(t+h|t), h = 0, 1, \ldots, N_p - 1\}. \end{cases} \tag{28}$$

Based on the Equation (17), we can deduce the whole system state equation in all predicted time:

$$\boldsymbol{X}_j = \boldsymbol{M}_\psi \boldsymbol{e}_j(t|t) + \boldsymbol{M}_B \boldsymbol{U}_j + \boldsymbol{M}_W \boldsymbol{W}_j, \tag{29}$$

where

$$\boldsymbol{M}_\psi = \text{col}\left\{\boldsymbol{G}_\psi^h, h = 1, 2, \ldots, N_p\right\}, \tag{30}$$

$$\boldsymbol{M}_B = \begin{bmatrix} \boldsymbol{G}_B & \boldsymbol{0} & \boldsymbol{0} & \cdots & \boldsymbol{0} \\ \boldsymbol{G}_\phi \boldsymbol{G}_B & \boldsymbol{G}_B & \boldsymbol{0} & \cdots & \boldsymbol{0} \\ \boldsymbol{G}_\phi^2 \boldsymbol{G}_B & \boldsymbol{G}_\phi \boldsymbol{G}_B & \boldsymbol{G}_B & \cdots & \boldsymbol{0} \\ \vdots & \vdots & \vdots & \vdots & \vdots \\ \boldsymbol{G}_\phi^{N_p-1} \boldsymbol{G}_B & \boldsymbol{G}_\phi^{N_p-2} \boldsymbol{G}_B & \boldsymbol{G}_\phi^{N_p-3} \boldsymbol{G}_B & \cdots & \boldsymbol{G}_B \end{bmatrix}, \tag{31}$$

$$\boldsymbol{M}_W = \begin{bmatrix} \boldsymbol{G}_W & \mathbf{0} & \mathbf{0} & \cdots & \mathbf{0} \\ \boldsymbol{G}_\phi \boldsymbol{G}_W & \boldsymbol{G}_W & \mathbf{0} & \cdots & \mathbf{0} \\ \boldsymbol{G}_\phi^2 \boldsymbol{G}_B & \boldsymbol{G}_\phi \boldsymbol{G}_W & \boldsymbol{G}_W & \cdots & \mathbf{0} \\ \vdots & \vdots & \vdots & \vdots & \vdots \\ \boldsymbol{G}_\phi^{N_p-1} \boldsymbol{G}_W & \boldsymbol{G}_\phi^{N_p-2} \boldsymbol{G}_W & \boldsymbol{G}_\phi^{N_p-3} \boldsymbol{G}_W & \cdots & \boldsymbol{G}_W \end{bmatrix}. \tag{32}$$

The feedback control strategy (25) can be rewritten as:

$$\boldsymbol{a}_j = \boldsymbol{K}\boldsymbol{X}_j + \boldsymbol{U}_j, \tag{33}$$

where

$$\boldsymbol{K} = \operatorname{diag}\left\{\boldsymbol{k}_j, h = 1, 2, \ldots, N_p\right\}.$$

Furthermore, the overall constraint of platoon j overall prediction slots N_p can be written as:

$$\begin{cases} \mathbb{X} = \left\{\boldsymbol{X} : \boldsymbol{X}_j^{\min} \le \boldsymbol{X}_j \le \boldsymbol{X}_j^{\max}\right\}; \\ \mathbb{U} = \left\{\boldsymbol{U} : \boldsymbol{U}_j^{\min} \le \boldsymbol{K}\boldsymbol{X}_j + \boldsymbol{U}_j \le \boldsymbol{U}_j^{\max}\right\}. \end{cases} \tag{34}$$

where

$$\boldsymbol{X}_j^{\min} = \operatorname{col}\left\{\boldsymbol{e}_j^{\min}, h = 1, 2, \ldots, N_p\right\},$$

$$\boldsymbol{X}_j^{\max} = \operatorname{col}\left\{\boldsymbol{e}_j^{\max}, h = 1, 2, \ldots, N_p\right\},$$

$$\boldsymbol{U}_j^{\min} = \operatorname{col}\left\{\boldsymbol{a}_j^{\min}, h = 1, 2, \ldots, N_p\right\},$$

$$\boldsymbol{U}_j^{\max} = \operatorname{col}\left\{\boldsymbol{a}_j^{\max}, h = 1, 2, \ldots, N_p\right\}.$$

Now, by letting

$$\begin{cases} \boldsymbol{Q}_X = \operatorname{diag}\{\underbrace{\boldsymbol{Q}, \ldots, \boldsymbol{Q}}_{N_p-1}, \boldsymbol{Q}_N\}; \\ \boldsymbol{R}_\alpha = \operatorname{diag}\{\underbrace{\boldsymbol{R}, \ldots, \boldsymbol{R}}_{N_p}\}, \end{cases} \tag{35}$$

and defining the unprocessed original model with uncertain perturbation for platoon j has the following form:

$$\min_{\boldsymbol{U}_j} \operatorname*{Exp}_{\boldsymbol{W}_j \in \mathrm{Ball}_\Phi} \left[\boldsymbol{X}_j^{\mathrm{T}} \boldsymbol{Q}_X \boldsymbol{X}_j + \boldsymbol{U}_j^{\mathrm{T}} \boldsymbol{R}_U \boldsymbol{U}_j\right] \tag{36a}$$

$$\text{s.t. } \boldsymbol{X}_j = \boldsymbol{M}_A \boldsymbol{e}_j(t|t) + \boldsymbol{M}_B \boldsymbol{U}_j + \boldsymbol{M}_W \boldsymbol{W}_j, \tag{36b}$$

$$\boldsymbol{X}_j \in \mathbb{X}, \forall\, \boldsymbol{W}_j \in \mathbb{W}, \tag{36c}$$

$$\boldsymbol{U}_j \in \mathbb{U}, \forall\, \boldsymbol{W}_j \in \mathbb{W}. \tag{36d}$$

For each platoon j, we develop the above optimization model to enable real-time control of the vehicles within the platoon. Specifically, in the presence of uncertain disturbances, we use the expected value of the value function as the optimization objective, while satisfying the uncertain state and control constraints to achieve robust control of each platoon. However, the model (36) is computationally difficult to handle due to the stochastic disturbances. The next work of this paper is to derive a computationally tractable equivalent framework for Model (36) based on robust equivalence theory.

C. Robust Counterpart Framework of Model (36) under Ball uncertain set

In this section, we deduce the robust counterpart framework for Model (36) under the scope of the Ball uncertain set. Uncertainty, an inherent feature in real-world systems, can significantly influence the behavior and performance of control systems. In the context of our study, the Ball uncertain set provides a structured way to encapsulate such uncertainties [47], [48]. Within this framework, our primary focus is to derive robust counterparts for both state constraints and control constraints. These robust counterparts ensure that our model remains computationally feasible even in the presence of uncertainties. By the following theorem, we provide robust equivalences for uncertain constraints.

Theorem 1: Given a metric $\boldsymbol{\Phi}$ under the Ball uncertain set, the robust counterpart framework of the state constraints $\boldsymbol{X}_j^{\min} \le \boldsymbol{X}_j \le \boldsymbol{X}_j^{\max}$ is:

$$C_{j,1}: \begin{cases} \boldsymbol{M}_B \boldsymbol{U}_j + \boldsymbol{\Phi}\sqrt{(\boldsymbol{M}_W)^2} \le \boldsymbol{X}_j^{\max} - \boldsymbol{M}_\psi \boldsymbol{e}_j(t|t); \\ -\boldsymbol{M}_B \boldsymbol{U}_j + \boldsymbol{\Phi}\sqrt{(-\boldsymbol{M}_W)^2} \le -\boldsymbol{X}_j^{\min} + \boldsymbol{M}_\psi \boldsymbol{e}_j(t|t). \end{cases} \tag{37}$$

Theorem 2: Given a metric $\boldsymbol{\Phi}$ under the Ball uncertainty set, the robust counterpart framework of the control constraint $\boldsymbol{U}_j^{\min} \le \boldsymbol{K}\boldsymbol{X}_j + \boldsymbol{U}_j \le \boldsymbol{U}_j^{\max}$ is:

$$C_{j,2}: \begin{cases} \boldsymbol{F}\boldsymbol{U}_j + \boldsymbol{\Phi}\sqrt{(\boldsymbol{K}\boldsymbol{M}_W)^2} \le \boldsymbol{U}_j^{\max} - \boldsymbol{K}\boldsymbol{M}_\psi \boldsymbol{e}_j(t|t); \\ -\boldsymbol{F}\boldsymbol{U}_j + \boldsymbol{\Phi}\sqrt{(-\boldsymbol{K}\boldsymbol{M}_W)^2} \le -\boldsymbol{U}_j^{\min} + \boldsymbol{K}\boldsymbol{M}_\psi \boldsymbol{e}_j(t|t). \end{cases} \tag{38}$$

where $\boldsymbol{F} = (\boldsymbol{K}\boldsymbol{M}_B + \boldsymbol{I})$.

For the proofs of Theorem 1 and Theorem 2, please refer to Appendices A and B, respectively. Thus, we derive a computationally tractable robust counterpart model for Model (36) under the Ball uncertainty set, which has the following concrete form:

$$\begin{aligned} \min_{\boldsymbol{U}_j} \ & \left[\overline{\boldsymbol{X}}_j^{\mathrm{T}} \boldsymbol{Q}_X \overline{\boldsymbol{X}}_j + \boldsymbol{U}_j^{\mathrm{T}} \boldsymbol{R}_U \boldsymbol{U}_j\right] \\ \text{s.t. } & C_{j,1} \text{ and } C_{j,2}. \end{aligned} \tag{39}$$

It can be observed that model (39) is a computationally solvable semi-definite programming model. Convex optimization algorithms, such as Sequential Quadratic Programming, can effectively solve this model. Next, we devise a robust control algorithm based on the foundation of solving the platoon formation model and the robust control model (Algorithm 1).

D. Computational Complexity Analysis

For the proposed RMPC model (36) of each platoon, the presence of uncertain perturbations makes the state update equations and corresponding constraints intractable. To overcome this problem, we construct a spherical uncertainty set based on robust optimization theory, and under this uncertainty set, we derive a computationally tractable equivalent form (39) of the model (36). In the framework of **Algorithm 1**, the computational burden is mainly generated by the RMPC of each platoon. In our setting, the data collection and platoon formation decisions are obtained offline, thus the computational efficiency of the algorithm depends on the choice of prediction time domain and control time domain on the RMPC

Algorithm 1: The Algorithm of RMPC

Input: Compute optimal platoon numbers y_j^*, vehicle sequences x_{ji}^* and platoon travel speed v_j^* by the model (9)

Obtain the feedback gain $\boldsymbol{K}$ offline;
Construct the Ball uncertain set and determine the measure Φ;
Select prediction time domain N_p;
for $j \in \mathcal{K}_i$ **do**
  Measure the initial state error $\boldsymbol{e}_j(t|t)$;
  Generate stochastic disturbances $\boldsymbol{W}_j$ of measure Φ under a fixed distribution;
  while $t \leq T$ **do**
    Compute optimal solution $\boldsymbol{U}_j$ by model (39);
    Generate the actual control $\boldsymbol{a}_j^* = \boldsymbol{K}\boldsymbol{X}_j + \boldsymbol{U}_j^*$;
    Implement the first step control $\boldsymbol{a}_j^*(t|t)$;
    Update $t = t + 1$;
  end
end

Output: the vehicle acceleration $\boldsymbol{a}_j^*$ in platoon j.

model. At each rolling horizon optimization, feedback control is triggered, and **Algorithm 1** is executed to obtain the control signal of all following vehicles. From the above analysis, it can be concluded that the computational complexity of the proposed algorithm depends on the number of constraints $C_{j,1}$ and $C_{j,2}$. Assume that the number of vehicles in platoon j is N_{veh} and the prediction time domain is N_p, then the number of $C_{j,1}$ and $C_{j,2}$ are $8N_{veh}N_p$ and $4N_{veh}N_p$. In Section IV below, we will demonstrate the computational efficiency of **Algorithm 1** to illustrate the real-time capability of the proposed algorithm.

TABLE I
PARAMETER SETTINGS IN OPTIMAL PLATOON FORMATION MODEL

Symbol	Value
Number of all vehicles	n = 20
Heavy vehicles	H = 6
Medium vehicles	M = 7
Light vehicles	L = 7
Number of candidate platoons	m = 5
Maximum number of platoons	k = 5
A sufficiently large number	$G = 1\times10^6$
Minimum vehicle number in platoon	$z_{\min} = 5\,veh$
Maximum vehicle number in platoon	$z_{\max} = 7\,veh$
Minimum speed of a platoon	$v_{\min} = 15\,m/s$
Maximum speed of a platoon	$v_{\max} = 40\,m/s$

VI. Simulation Results

In this section, we conduct simulation experiments to verify the effectiveness of the proposed framework. First, we introduce the data collection process and calculate the average speed for each vehicle. Subsequently, using the proposed optimal platoon-forming strategy, we form multiple platoons

TABLE II
PARAMETER SETTINGS OF PLATOON CONTROL

Symbol	Value
Minimum vehicle acceleration in platoon	$a_i^{\min}$ = -3 m/s^2
Maximum vehicle acceleration in platoon	$a_i^{\max}$ = 3 m/s^2
Minimum velocity error	$e_{v,i}^{\min}$ = -2 m/s
Maximum velocity error	$e_{v,i}^{\max}$ = 2 m/s
Minimum spacing error	$e_{p,i}^{\min}$ = 0 m
Maximum spacing error	$e_{p,i}^{\max}$ = 3 m
Desired vehicle distance	D = 10 m
Prediction time domain	N_p = 3 s
Control time domain	N_c = 0.5 s
Time interval	τ = 0.5 s
Reaction time	r = 0.5 s
Vehicle length	L = 2 m

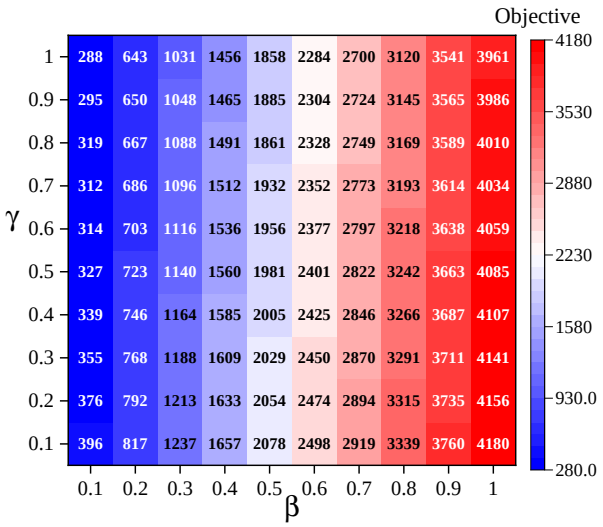

Fig. 3. The utility estimates under different utility parameters β and γ.

of 20 vehicles of various types. We then observe the effects of different negative benefit parameters, γ and β, on platoon formation to select the appropriate weight parameters that maximize the benefit of all platoons. In the third step, we implement a centralized robust platoon controller in the lead vehicle of each platoon. This controller counteracts the effects of uncertain noise from V2V communication on the stability of the platoon system, enhancing the safety and resilience of the vehicle platoon. Additionally, we implement all simulations in Matlab/Simulink-based solver version R2020, running on a 2.8-GHz 64-bit Core i7-8400U CPU machine under Windows 10 Professional.

A. Data Collection

Vehicle data collection uses its traffic status information on fixed road segments. In this initial phase, we calculate the speed of each vehicle traveling individually on a fixed road segment through the California Traffic Performance Measurement System [49]. Through the vehicle detection station in this system, we can obtain the vehicle density, number of vehicles

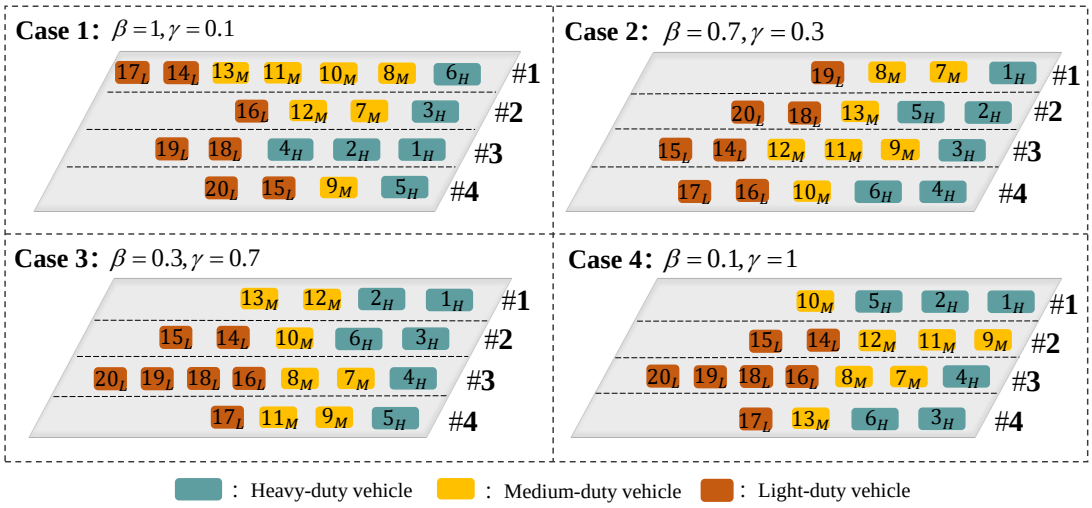

Fig. 4. The optimal platoon formation under four cases.

TABLE III
THE UTILITY OBJECTIVES AND OPTIMAL VELOCITY OF FOUR CASES

	Case 1		**Case 2**		**Case 3**		**Case 4**	
	$\beta=1$	$\gamma=0.1$	$\beta=0.7$	$\gamma=0.3$	$\beta=0.3$	$\gamma=0.7$	$\beta=0.1$	$\gamma=1$
Platoon1 optimal speed	v_1^*=15 m/s		v_1^*=15 m/s		v_1^*=15 m/s		v_1^*=15 m/s	
Platoon2 optimal speed	v_2^*=15 m/s		v_2^*=15 m/s		v_2^*=18.6 m/s		v_2^*=31 m/s	
Platoon3 optimal speed	v_3^*=15 m/s		v_3^*=15 m/s		v_3^*=40 m/s		v_3^*=40 m/s	
Platoon4 optimal speed	v_4^*=15 m/s		v_4^*=15 m/s		v_4^*=15 m/s		v_4^*=21 m/s	
Total valuation	$U(v_j^*, y_j^*, x_{ij}^*)$=**4180.00**		$U(v_j^*, y_j^*, x_{ij}^*)$=2870.11		$U(v_j^*, y_j^*, x_{ij}^*)$=1096.25		$U(v_j^*, y_j^*, x_{ij}^*)$=287.62	

and average speed of vehicles in a fixed road section [50]. Finally, the vehicle information of this road section is uploaded to the cloud to generate corresponding decisions. The individual driving speeds of 20 vehicles are: $\mathbf{v} = [v^1, \ldots, v^{20}]$ = [15 m/s, 18 m/s, 17 m/s, 23 m/s, 13 m/s, 20 m/s, 31 m/s, 24 m/s, 34 m/s, 28 m/s, 31 m/s, 30 m/s, 25 m/s, 32 m/s, 35 m/s, 40 m/s, 41 m/s, 29 m/s, 38 m/s, 35 m/s].

B. Optimal Platoon Formation

In this subsection, we aim to identify optimal platoon formations in a traffic system consisting of 20 vehicles. The system comprises 6 heavy vehicles, 7 medium vehicles, and 7 light vehicles. For clarity, all vehicles are numbered sequentially from heavy to light (i = 1, …, 20). We denote the vehicle types as H, M, and L, respectively [15]. The basic parameters are given in Table I. Besides, there are 5 candidate platoons in the system, and the values of $\alpha_{ji,1}$, $\alpha_{ji,2}$ and $\alpha_{ji,3}$ in each platoon are:

$$\begin{aligned}
&\alpha_{1i,1}=0.6, \alpha_{1i,2}=0.2, \alpha_{1i,2}=0.3;\\
&\alpha_{2i,1}=0.7, \alpha_{2i,2}=0.5, \alpha_{2i,2}=0.3;\\
&\alpha_{3i,1}=0.5, \alpha_{3i,2}=0.3, \alpha_{3i,2}=0.2;\\
&\alpha_{4i,1}=0.7, \alpha_{4i,2}=0.2, \alpha_{4i,2}=0.5;\\
&\alpha_{5i,1}=0.9, \alpha_{5i,2}=0.4, \alpha_{5i,2}=0.3.
\end{aligned} \tag{40}$$

Numerical results in Figure 3 show the total utility estimates of all platoons under different parameters β and γ. We can observe that when the fuel consumption weight coefficient β increases, the utility value (that is, the willingness value of the vehicle i to join the formation j) will increase, and when the negative utility weight coefficient γ increases, the utility value will decrease. In order to further observe and select the appropriate parameters to maximize the benefits of platoon forming, we identified 4 platoons among all candidate rows, as shown in Figure 4. This figure contains the total number of vehicles in each platoon and the number of each type of vehicle in the platoon, where subscripts denote specific vehicle types (e.g., "12_M" signifies a medium-sized vehicle with the serial number 12). Additionally, Table III lists the optimal solutions for every platoon, including the optimal speed v_j and utility estimates $U(v_j^*, y_j^*, x_{ji}^*)$. From the observations in Figure 4 and Table III, it is evident that the overall utility is the largest under the optimal platoon formation sequence of $\beta = 1$ and $\gamma = 0.1$, with all four platoons traveling at 15 m/s.

C. Control Performance Verification

Through the above-mentioned macro architecture of vehicle multi-formation based on economy, we will design a centralized robust controller for each platoon to cope with the stochastic noise in the traffic environment. It is evident from the preceding section that the platoon comprising 20 vehicles

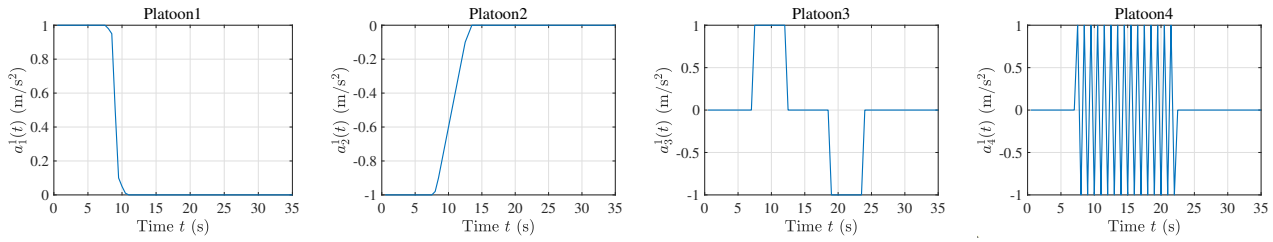

(a) Acceleration of vehicle 6_H (b) Acceleration of vehicle 3_H (c) Acceleration of vehicle 1_H (d) Acceleration of vehicle 5_H

Fig. 5. The leading vehicle accelerations of four platoon.

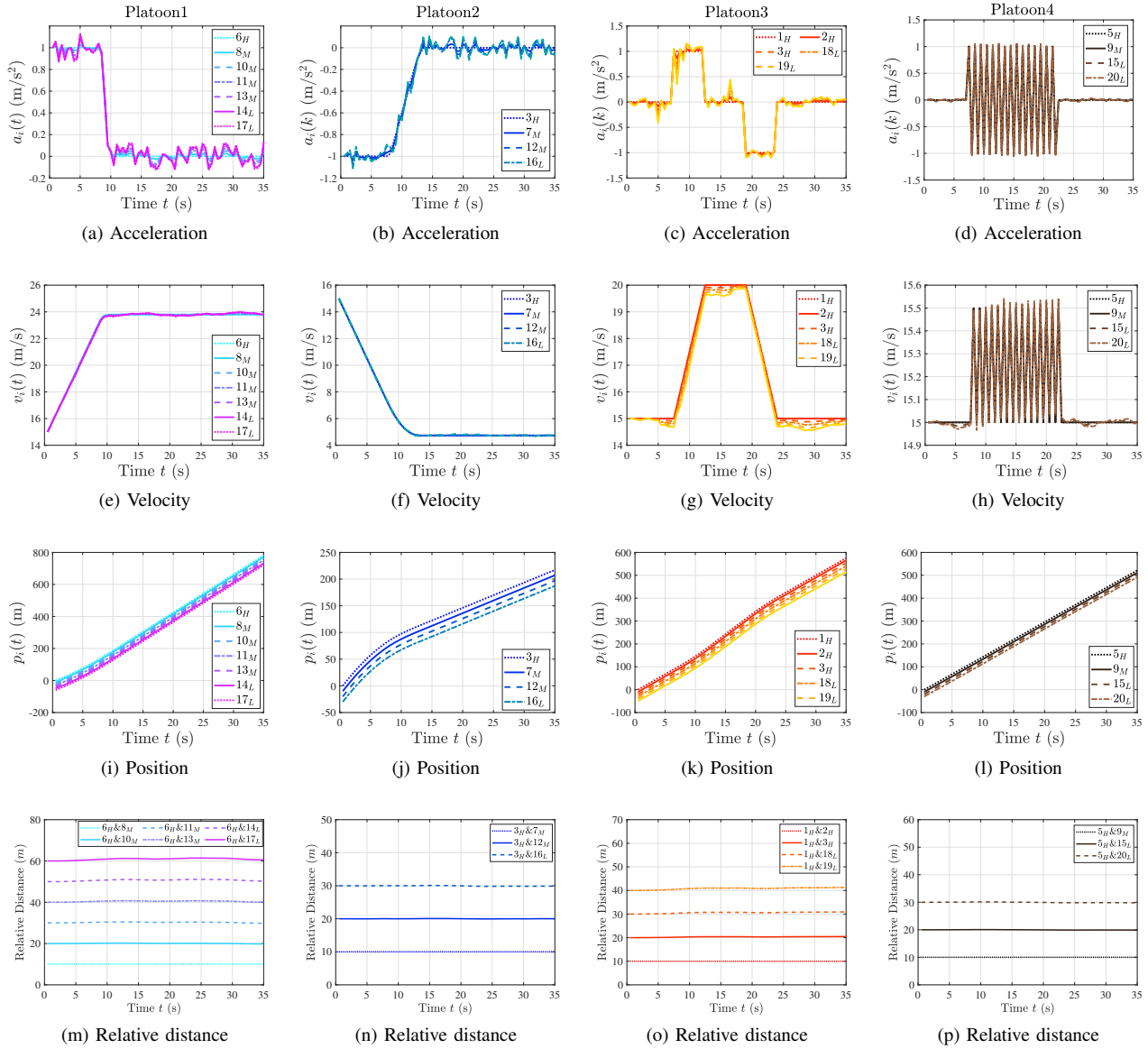

(a) Acceleration (b) Acceleration (c) Acceleration (d) Acceleration

(e) Velocity (f) Velocity (g) Velocity (h) Velocity

(i) Position (j) Position (k) Position (l) Position

(m) Relative distance (n) Relative distance (o) Relative distance (p) Relative distance

Fig. 6. The acceleration, velocity, position and relative distance of the vehicles in 4 platoons. First row: Platoon1, Second row: Platoon2, Third row: platoon3, Fourth row: Platoon4.

in Case 1 ($\beta = 1$ and $\gamma = 0.1$) yields the utmost utility value. Consequently, we shall devise a centralized robust controller for each optimal platoon. Specifically, the initial velocity of the four optimal formations is set at $15\,m/s$, while the initial position of the vehicles in each formation is randomly generated within the range of [-100, 0] m. Moreover, the initial acceleration of all vehicles in the formation is set to $0\,m/s^2$. Furthermore, each formation's controller is positioned on the lead vehicle, and the motion state of the leading vehicle is known within a time frame of [0, 35] s. As depicted in Figure 5, we provide the acceleration of the leading vehicle in the four formations. It is important

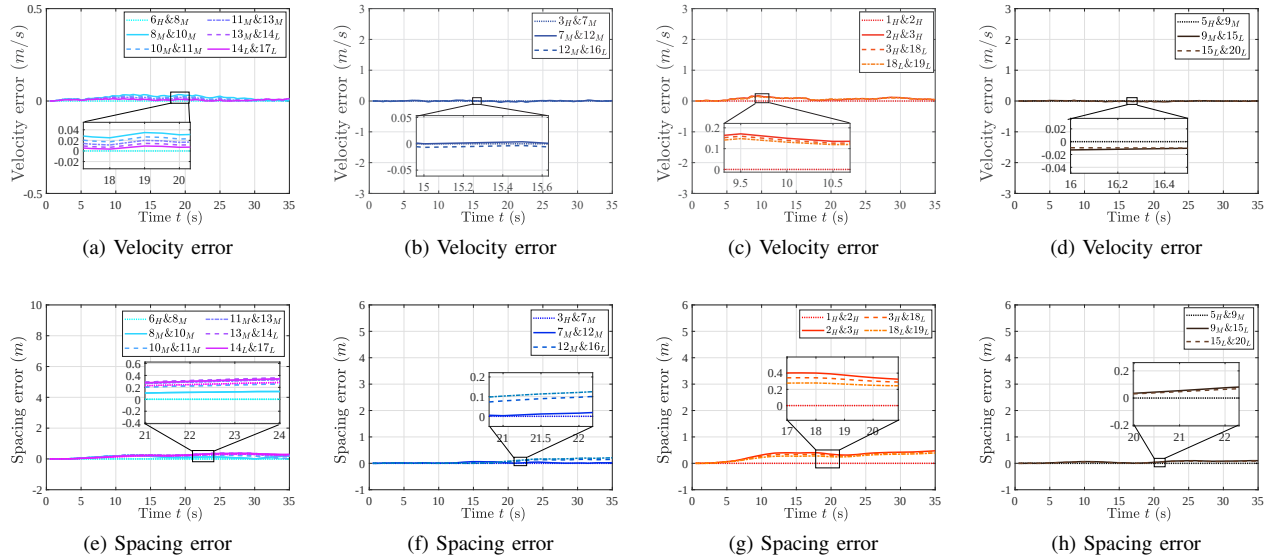

(a) Velocity error (b) Velocity error (c) Velocity error (d) Velocity error

(e) Spacing error (f) Spacing error (g) Spacing error (h) Spacing error

Fig. 7. The velocity error and spacing error of the vehicles. First row: Platoon1, Second row: Platoon2, Third row: platoon3, Fourth row: Platoon4.

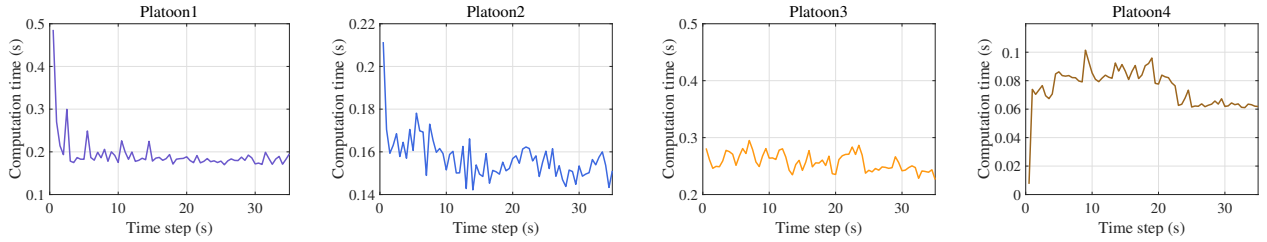

(a) Computation time (b) Computation time (c) Computation time (d) Computation time

Fig. 8. The computational efficiency of robust platoon controllers.

to note that we assign distinct acceleration profiles to each platoon to assess whether the proposed platoon controller can maintain stability for trailing vehicles across different driving conditions, such as frequent acceleration and deceleration. The remaining parameter settings for platoon control are provided in Table II.

In order to verify the effectiveness of the proposed platoon control method, we conduct simulation experiments on different types of external stochastic disturbances. For platoon1, the stochastic disturbance $w_1^i(t)$ obeys the Uniform distribution, that is, $w_1^i(t) \sim U(-0.02, 0.02)$; For platoon2, the stochastic disturbance $w_2^i(t)$ obeys the Uniform distribution, that is, $w_2^i(t) \sim U(-0.05, 0.05)$; For platoon3, the stochastic disturbance $w_3^i(t)$ obeys the Gaussian distribution, that is, $w_3^i(t) \sim N(0, 0.01)$; For platoon4, the stochastic disturbance $w_4^i(t)$ obeys the Gaussian distribution, that is, $w_4^i(t) \sim N(0, 0.03)$.

The effect of the platoon controllers is shown in Figure 6. In Figure 6, we plot the vehicle acceleration, velocity and position generated by each platoon under the robust controller. From the sub-figures (6a)-(6d), it can be seen that the acceleration of all following vehicles is strictly limited within the set interval [-3 m/s^2, 3 m/s^2] in the presence of stochastic disturbances. It can be observed from sub-figures (6e)-(6h) that platoons 1-4 track the speed of the leading vehicle stably after 10 s, 12 s, 24 s and 22 s respectively, that is, travel at the expected speed 15 m/s. From sub-figures (6i) and (6l), it can be analyzed that even in the traffic environment with stochastic disturbances, the vehicles in each platoon can form a stable formation, travel at a fixed distance and a stable speed without any chain collisions. Besides, we also show the position information of the following vehicle relative to the leader. It can be seen from the subfigures (6m)-(6p) that the distance between vehicles in platoons 1-4 is stable at D=10 m. The above experimental results show that the proposed platoon controller can guarantee the safety and robustness of the following vehicle no matter whether the leading vehicle is driving under acceleration, deceleration, periodic acceleration/deceleration or frequent acceleration/deceleration.

In Figure 7, we illustrate the velocity and inter-vehicle spacing errors between two consecutive vehicles in four platoons under the robust control strategy. It is evident from sub-figures (7a)-(7d) that the following vehicles in all platoons can track the time-varying expected speed of the leading vehicle. Even when the driving state of the leading vehicle changes suddenly, such as during emergency acceleration or deceleration, the following vehicles in each platoon remain controlled close to the expected speed. In addition, we can also realize that the speed consistency of formation vehicles is guaranteed even in the presence of stochastic disturbances. Sub-figures

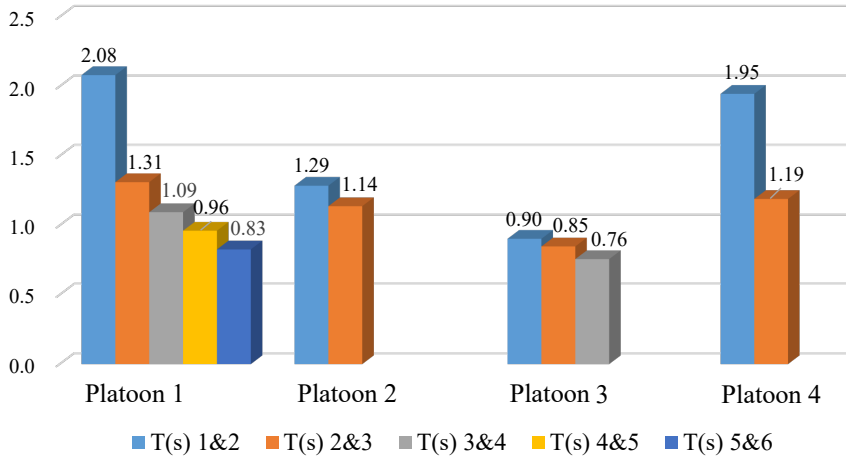

Fig. 9. The string amplitude value of four platoons in the frequency domain.

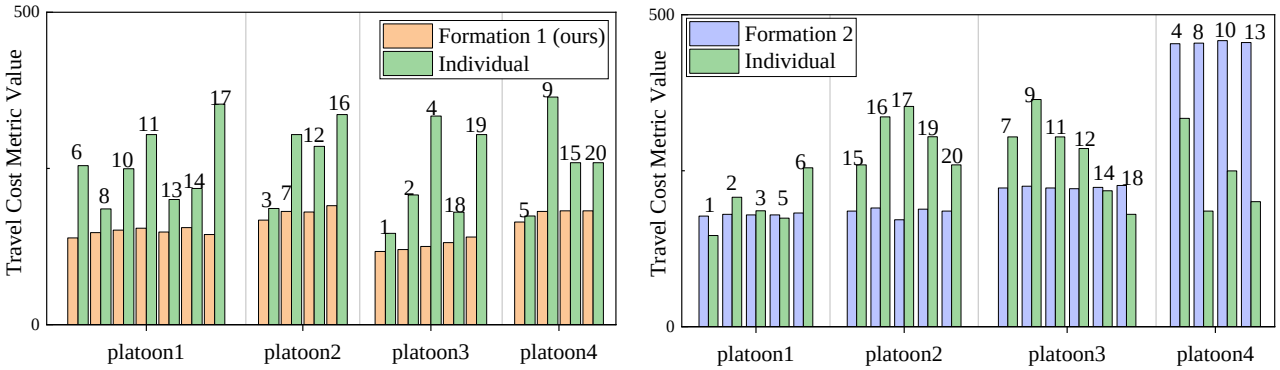

(a) Formation 1 cost and the vehicle's individual cost

(b) Formation 2 cost and the vehicle's individual cost

Fig. 10. Comparison of travel cost metric value when vehicles travel individually and when vehicles travel in platoons (The lower the cost, the more stable the convoy behavior).

(7e)-(7h) demonstrate the spacing error between two consecutive vehicles in four platoons. The discernible observation is that, despite the influence of stochastic disturbances on the formation system, the vehicle spacing error in each platoon consistently remains above $0\,m$. This compellingly demonstrates the efficacy of the proposed robust control strategy, which diligently guarantees the platoon's safety and effectively mitigates the potential risks of chain collisions among the following vehicles.

Furthermore, we show the computational efficiency of four platoons under the proposed centralized RMPC method in Figure 8. When the prediction time domain $N_p = 3.5\,s$ and the control time domain $N_c = 0.5\,s$ are selected, the execution time of Algorithm 1 can be effectively completed within the control time domain, and the average calculation times of the four platoons are $0.19\,s$, $0.15\,s$, $0.25\,s$, and $0.07\,s$ respectively. These experimental results demonstrate that the proposed centralized control algorithm effectively ensures timely and responsive decision-making within each platoon, facilitating smooth and efficient fleet operations. By completing the execution of Algorithm 1 within the designated control time domain, the controller demonstrates its capability to meet stringent real-time requirements, essential for ensuring safe and reliable platooning maneuvers on highways.

Given the introduction of uncertain measurement errors in platoon systems, traditional time-domain string stability analysis becomes challenging. Hence, we adopt a frequency domain approach to evaluate local string stability under stochastic disturbances [51]. First, we apply the Discrete Fourier Transform function to the spacing error $\triangle e^j_{p,i}(t)$ and the transfer function is $\Xi^j_i(s) = \sum_t \triangle e^j_{p,i}(t) \exp^{-s\eta t}$, where $s \in [0, \pi], \eta = \sqrt{-1}$. Then, we introduce a metric function $T_i(s) = |\frac{\Xi^j_i(s)}{\Xi^j_{i-1}(s)}|$, defined as the absolute value of the ratio of Fourier transforms of spacing errors between adjacent vehicles. If $T_i(s)$ exhibits a decreasing trend along the platoon, it indicates the string stability of the platooning system under the RMPC method in the frequency domain. We calculate the amplitude of each vehicle through the transfer function of the spacing error and obtain the string amplitude of the spacing error. As shown in Figure 9, we show the amplitudes of four strings arranged in the frequency domain. It can be seen that $T_i(s)$ gradually decreases from the beginning to the end of the platoon. This shows that the proposed robust platoon controller has strong robustness under different stochastic disturbances, and the string stability of the vehicle platoon system is guaranteed.

TABLE IV
THE TRAVEL COST METRIC VALUE UNDER FORMATION 1, FORMATION 2 AND VEHICLES TRAVEL INDIVIDUALLY

	Platoon1	Platoon2	Platoon3	Platoon4		Platoon1	Platoon2	Platoon3	Platoon4
Optimal Speed	$15\,m/s$	$15\,m/s$	$15\,m/s$	$15\,m/s$	Optimal Speed	$17\,m/s$	$15\,m/s$	$20\,m/s$	$20\,m/s$
Individual Cost	1764.7	1111.7	1171.9	993.8	Individual Cost	904.8	1512.1	1656	**969.2**
Formation 1 Cost	**1059.7**	**719.2**	**634**	**709.8**	Formation 2 Cost	**897.5**	**920.5**	**1340.2**	1822

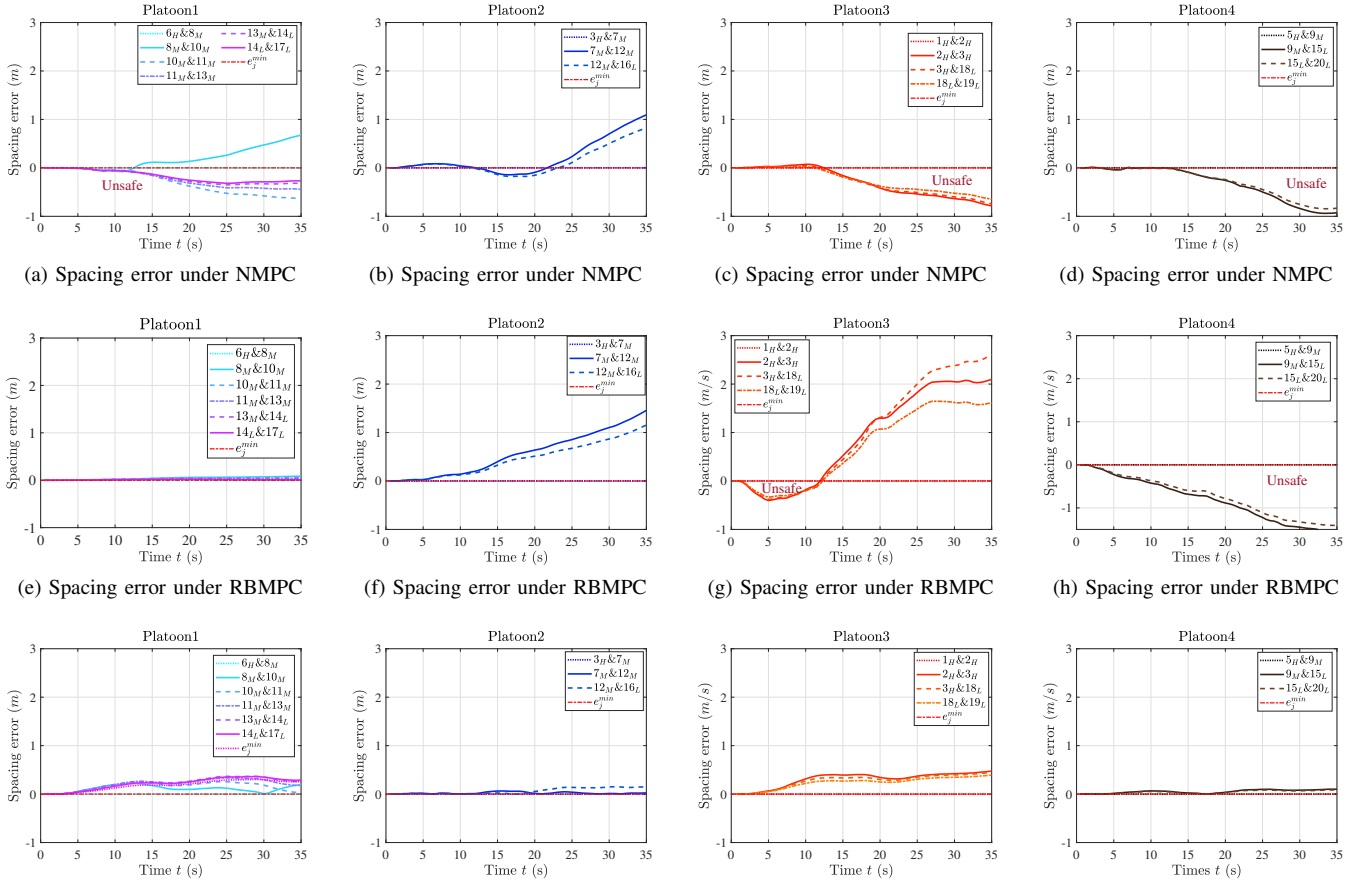

(a) Spacing error under NMPC (b) Spacing error under NMPC (c) Spacing error under NMPC (d) Spacing error under NMPC

(e) Spacing error under RBMPC (f) Spacing error under RBMPC (g) Spacing error under RBMPC (h) Spacing error under RBMPC

(i) Spacing error under RMPC (Ours) (j) Spacing error under RMPC (Ours) (k) Spacing error under RMPC (Ours) (l) Spacing error under RMPC (Ours)

Fig. 11. The spacing error of every platoon under NMPC, RBMPC and RMPC methods.

VII. COMPARISON EXPERIMENT

We conduct a comparative experiment on two aspects. Firstly, we evaluate the travel costs of vehicles traveling under different platoon formation strategies versus traveling independently. The evaluation aims to illustrate the advantages of the proposed optimal platooning strategy in terms of vehicle behavior and fuel economy. Secondly, at the macroscopic level, we compare the proposed ball-based RMPC method with the nominal robust control method (without interference immunity) and the robust bounded control method to verify that the RMPC model can improve the impact of stochastic disturbances.

A. Platoon Valuation

In this section, we aim to vehicle travel costs under three formations: Economic-based formation driving (Formation 1), formation driving without considering economy (Formation 2) and independent driving. This assessment seeks to validate the advantages of the proposed optimal platoon formation model in terms of vehicle cohesion. The specific settings in the three cases are $\beta = 1$ and $\gamma = 0.1$, $\beta = 0.001$ and $\gamma = 1$, $\beta = 1$. Correspondingly, we define the travel cost metric function of platoon j as:

$$Metric_j^F = \sum_{i \in \mathcal{M}_j} [\alpha_{ji,1}(v_j^*)^2 + \alpha_{ji,2} v_j^* + \alpha_{ji,3}] y_j^* + \left| v_j^* - v_i \right|, \tag{41}$$

and we can obtain the metric value of the vehicle traveling alone by solving Equation (1). Formation 1 and Formation 2 will produce two different vehicle formation situations, so we use two figures to show the formation composition and corresponding travel costs under the three strategies. Figure (10a) compares the cost value under the economic-based vehicle pla-

toon driving and vehicle driving alone. Figure (10b) compares the cost value under the non-economic vehicle platoon driving and vehicle driving alone. It can be seen from the two figures that the vehicle travel cost under Formation 1 (ours) is always less than the vehicles traveling alone, however in Formation 2 the cost of vehicles traveling in a platoon is higher than the cost of traveling alone. For example, the overall cost of Platoon 4 is higher than the cost of traveling alone, which will lead to poor cohesion and unstable behavior of vehicles in Platoon 4, and this platoon will face the risk of disbandment. Table IV shows travel cost metric value under Formation 1, Formation 2 and vehicles travel individually. From numerical analysis, the travel costs of the four platoons under the economic-based multi-platoon forming strategy (Formation 1) are reduced by 39.95%, 35.30%, 45.89% and 28.57% respectively compared with the cost of traveling alone. Upon examination, the following conclusions can be drawn: the proposed platoon formation method always lowers the travel cost of vehicles traveling in a platoon than the estimates from their independent driving. Consequently, individual vehicles have no incentive to depart from the platoon, affirming the behavioral stability of the four platoon systems established.

B. Ablation Study

In this subsection, we conduct a comparative experiment to show the advantage of the safety and robustness inherent in our proposed RMPC method, the Robust Bound (Min-max) control method (RBMPC) and the Nominal MPC method (NMPC). Firstly, with parameters set at $\beta = 1$ and $\gamma = 0.1$, we determine the optimal platoon count number for the sequence of vehicles within each platoon. Following this determination, our ablation analysis is initiated, primarily aimed at contrasting the interference suppression abilities of the RMPC, RBMPC and NMPC methods. The design idea of the RBMPC model is based on reference [33], we assume that there are upper and lower bounds for uncertain disturbances, and solve the vehicle acceleration at the boundaries of the disturbance based on the worst-case principle. Besides, the RMPC model is presented through model (15) and the NMPC model is shown below:

$$\begin{aligned}
\min_{\boldsymbol{U}_j} \ & \left[\boldsymbol{X}_j^{\mathrm{T}}\boldsymbol{Q}_X\boldsymbol{X}_j + \boldsymbol{U}_j^{\mathrm{T}}\boldsymbol{R}_U\boldsymbol{U}_j\right] \\
\text{s.t. } & \boldsymbol{X}_j = \boldsymbol{M}_A\boldsymbol{e}_j(t|t) + \boldsymbol{M}_B\boldsymbol{U}_j, \\
& \boldsymbol{X}_j \in \mathbb{X}, \\
& \boldsymbol{U}_j \in \mathbb{U}.
\end{aligned}$$

We apply different levels of stochastic disturbances to the four resulting optimal platoons, i.e., $w_1^i(t) \sim U(-0.02, 0.02)$; $w_2^i(t) \sim U(-0.05, 0.05)$; $w_3^i(t) \sim N(0, 0.01)$; $w_4^i(t) \sim N(0, 0.03)$. Figure 11 shows the spacing error of every platoon under the RMPC method, RBMPC method and NMPC method. Specifically, as can be observed from subfigures (11a)-(11d), when the platoon system is subjected to stochastic disturbances, the inter-vehicle spacing error under the NMPC method exceeds the safety constraint threshold, indicating that the platoon exists potential risk of collision. Under the RBMPC method, we can find that the spacing errors of vehicles in platoons 1 and 2 are both greater than 0, and safety constraints are violated in platoons 3 and 4 (Subfigures 11e-11h). Although the driving safety of vehicles in Platoons 1 and 2 can be guaranteed under the RBMPC method, the distance between vehicles in Platoon 4 gradually decreases, which shows that there is a risk of collision in Platoon 4. This is not difficult to explain. The characteristics of stochastic disturbances in platoons 1 and 2 are stochastic perturbation. The proposed RBMPC can effectively improve the robustness of the system. However, when the stochastic disturbances have no boundary information but characteristic information (expectation and variance), the RBMPC method begins to violate safety constraints and cannot guarantee vehicle safety. It can be seen from subfigures (11i)-(11l), that the spacing error under the proposed RMPC method consistently remains above zero. For example, the average spacing error of Platoon 1 under the RMPC method is $0.1181\,m$, under the RBMPC method is $0.09342\,m$, and under the NMPC the mean spacing error is -$0.1173\,m$. In general, the NMPC method tends to decrease the spacing between consecutive vehicles, posing a risk of collision over extended driving durations. The RBMPC method can reduce the influence of bounded disturbances but cannot deal with uncertain disturbances with stochastic characteristics. Contrastingly, the RMPC method that we propose exhibits superior versatility and robustness. It is capable of effectively dealing with various types of uncertain disturbances, including those with stochastic characteristics. This enhanced capability enables the RMPC method to provide reliable and stable control over platoon formations, even in dynamically changing and unpredictable traffic environments. Furthermore, the experimental results underscore the effectiveness of the RMPC method in comparison to the NMPC and RBNPC methods. The RMPC method ensures enhanced vehicle safety and robustness within the platoon system by effectively counteracting uncertainties. This superior performance highlights the potential of the RMPC method to address the challenges posed by dynamic and unpredictable traffic conditions.

VIII. Conclusion

In this paper, we presented a robust model predictive control framework for the multi-lane platoons under the fuel economy principle. Our approach uniquely integrated a vehicle scheduling system and an online platoon control system to enhance the efficiency of platoon formations. Moreover, we introduced an optimal platoon formation model tailored for heterogeneous vehicle types, aiming to maximize platooning utility. This model innovatively decides on the number of platoons, the sequence of vehicles within the platoon, and the platoon speed. Through numerical analysis, we observed a substantial reduction in travel costs for platoons formed under the economic-based multi-platoon forming strategy, ensuring the behavioral stability and high cohesion of the platooning vehicles. Based on the above multi-formation structure, our study introduced a centralized robust controller for each platoon, designed to address complexities and uncertainties prevalent in vehicular dynamics and potential external disturbances. The RMPC method exhibited superior versatility and robustness, and effectively dealt with various types of uncertain

perturbations, including those with stochastic characteristics. Experimental results further validated the effectiveness of the RMPC method, showcasing its superiority over alternative methods such as NMPC and RBNPC.

In this initial study, we acknowledge that the research presented in this manuscript operates under certain assumptions, including a limited number of vehicles in the experiments. Moving forward, our future work will aim to address these limitations by expanding the scale of the experiments to include a larger number of vehicles, thereby providing a more comprehensive assessment of our approach. Additionally, we will explore the optimization problem of integrated scheduling and control in greater depth, including complex scenarios such as lane changing and the lateral and longitudinal control of vehicles within the platoon. By broadening our focus to encompass these aspects, we aim to enhance the robustness and applicability of our approach, ensuring it can effectively manage a wider range of real-world driving conditions.

APPENDIX A

For the state constraint $\boldsymbol{X}_j^{\min} \leq \boldsymbol{X}_j \leq \boldsymbol{X}_j^{\max}$, we write it as:

$$\begin{cases} X_j \leq \boldsymbol{X}_j^{\max}; \\ -X_j \leq -\boldsymbol{X}_j^{\min}. \end{cases} \tag{42}$$

Taking the equation $\boldsymbol{X}_j = \boldsymbol{M}_\psi \boldsymbol{e}_j(t|t) + \boldsymbol{M}_B \boldsymbol{U}_j + \boldsymbol{M}_W \boldsymbol{W}_j$ into the above equation, we can deduce:

$$\begin{cases} \boldsymbol{M}_\psi \boldsymbol{e}_j(t|t) + \boldsymbol{M}_B \boldsymbol{U}_j + \boldsymbol{M}_W \boldsymbol{W}_j \leq \boldsymbol{X}_j^{\max}; \\ -\boldsymbol{M}_\psi \boldsymbol{e}_j(t|t) - \boldsymbol{M}_B \boldsymbol{U}_j - \boldsymbol{M}_W \boldsymbol{W}_j \leq -\boldsymbol{X}_j^{\min}. \end{cases} \tag{43}$$

Due to the stochastic nature of $\boldsymbol{W}_j$, we can obtain:

$$\begin{cases} \boldsymbol{M}_W \boldsymbol{W}_j \leq \boldsymbol{X}_j^{\max} - \boldsymbol{M}_\psi \boldsymbol{e}_j(t|t) - \boldsymbol{M}_B \boldsymbol{U}_j; \\ -\boldsymbol{M}_W \boldsymbol{W}_j \leq -\boldsymbol{X}_j^{\min} + \boldsymbol{M}_\psi \boldsymbol{e}_j(t|t) + \boldsymbol{M}_B \boldsymbol{U}_j. \end{cases} \tag{44}$$

Based on the Worst-Case Principle (WCP) [48], the above inequality can be written as:

$$\begin{cases} \sup_{\|w_j^i(t)\|_2 \leq \Phi} [\boldsymbol{M}_W \boldsymbol{W}_j] \leq \boldsymbol{X}_j^{\max} - \boldsymbol{M}_\psi \boldsymbol{e}_j(t|t) - \boldsymbol{M}_B \boldsymbol{U}_j; \\ \sup_{\|w_j^i(t)\|_2 \leq \Phi} [-\boldsymbol{M}_W \boldsymbol{W}_j] \leq -\boldsymbol{X}_j^{\min} + \boldsymbol{M}_\psi \boldsymbol{e}_j(t|t) + \boldsymbol{M}_B \boldsymbol{U}_j. \end{cases}$$

$$\Downarrow \text{ (Theorem 1.3.4 by [47])}$$

$$\begin{cases} \boldsymbol{\Phi} \sqrt{(\boldsymbol{M}_W)^2} \leq \boldsymbol{X}_j^{\max} - \boldsymbol{M}_\psi \boldsymbol{e}_j(t|t) - \boldsymbol{M}_B \boldsymbol{U}_j; \\ \boldsymbol{\Phi} \sqrt{(-\boldsymbol{M}_W)^2} \leq -\boldsymbol{X}_j^{\min} + \boldsymbol{M}_\psi \boldsymbol{e}_j(t|t) + \boldsymbol{M}_B \boldsymbol{U}_j. \end{cases}$$

Proof of Theorem 1 is complete.

APPENDIX B

For the uncertain control constraint $\boldsymbol{U}_j^{\min} \leq \boldsymbol{a}_j \leq \boldsymbol{U}_j^{\max}$, we write it as:

$$\begin{cases} \boldsymbol{a}_j \leq \boldsymbol{U}_j^{\max}; \\ -\boldsymbol{a}_j \leq -\boldsymbol{U}_j^{\min}. \end{cases} \tag{45}$$

Taking the Equations $\boldsymbol{a}_j = \boldsymbol{K}\boldsymbol{X}_j + \boldsymbol{U}_j$ and $\boldsymbol{X}_j = \boldsymbol{M}_\psi \boldsymbol{e}_j(t|t) + \boldsymbol{M}_B \boldsymbol{U}_j + \boldsymbol{M}_W \boldsymbol{W}_j$ into the above equation, we can deduce:

$$\begin{cases} \boldsymbol{K}(\boldsymbol{M}_\psi \boldsymbol{e}_j(t|t) + \boldsymbol{M}_B \boldsymbol{U}_j + \boldsymbol{M}_W \boldsymbol{W}_j) + \boldsymbol{U}_j \leq \boldsymbol{U}_j^{\max} \\ -\boldsymbol{K}(\boldsymbol{M}_\psi \boldsymbol{e}_j(t|t) + \boldsymbol{M}_B \boldsymbol{U}_j + \boldsymbol{M}_W \boldsymbol{W}_j) + \boldsymbol{U}_j \leq -\boldsymbol{U}_j^{\min} \end{cases}$$

$$\Downarrow \boldsymbol{F} = (\boldsymbol{K}\boldsymbol{M}_B + \boldsymbol{I})$$

$$\begin{cases} \boldsymbol{K}\boldsymbol{M}_\psi \boldsymbol{e}_j(t|t) + \boldsymbol{F}\boldsymbol{U}_j + \boldsymbol{K}\boldsymbol{M}_W \boldsymbol{W}_j \leq \boldsymbol{U}_j^{\max} \\ -\boldsymbol{K}\boldsymbol{M}_\psi \boldsymbol{e}_j(t|t) - \boldsymbol{F}\boldsymbol{U}_j - \boldsymbol{K}\boldsymbol{M}_W \boldsymbol{W}_j \leq -\boldsymbol{U}_j^{\min} \end{cases}$$

$$\Downarrow \text{ (WPC)}$$

$$\begin{cases} \sup_{\|w_j^i(t)\|_2 \leq \Phi} [\boldsymbol{K}\boldsymbol{M}_W \boldsymbol{W}_j] \leq \boldsymbol{U}_j^{\max} - \boldsymbol{K}\boldsymbol{M}_\psi \boldsymbol{e}_j(t|t) - \boldsymbol{F}\boldsymbol{U}_j \\ \sup_{\|w_j^i(t)\|_2 \leq \Phi} [\boldsymbol{K}\boldsymbol{M}_W \boldsymbol{W}_j] \leq -\boldsymbol{U}_j^{\min} + \boldsymbol{K}\boldsymbol{M}_\psi \boldsymbol{e}_j(t|t) + \boldsymbol{F}\boldsymbol{U}_j \end{cases}$$

$$\Downarrow \text{ (Theorem 1.3.4 by [47])}$$

$$\begin{cases} \boldsymbol{F}\boldsymbol{U}_j + \boldsymbol{\Phi} \sqrt{(\boldsymbol{K}\boldsymbol{M}_W)^2} \leq \boldsymbol{U}_j^{\max} - \boldsymbol{K}\boldsymbol{M}_\psi \boldsymbol{e}_j(t|t) \\ -\boldsymbol{F}\boldsymbol{U}_j + \boldsymbol{\Phi} \sqrt{(-\boldsymbol{K}\boldsymbol{M}_W)^2} \leq -\boldsymbol{U}_j^{\min} + \boldsymbol{K}\boldsymbol{M}_\psi \boldsymbol{e}_j(t|t) \end{cases}$$

Proof of Theorem 2 is complete.

REFERENCES

[1] M. Muratori, J. Holden, M. Lammert, A. Duran, S. Young, and J. Gonder, "Potential for platooning in u.s. highway freight transport," *SAE International Journal of Commercial Vehicles*, vol. 10, 03 2017.

[2] D. Jia, K. Lu, J. Wang, X. Zhang, and X. Shen, "A survey on platoon-based vehicular cyber-physical systems," *IEEE Communications Surveys & Tutorials*, vol. 18, no. 1, pp. 263–284, 2016.

[3] J. Zhou, D. Tian, Z. Sheng, X. Duan, G. Qu, D. Cao, and X. Shen, "Decentralized robust control for vehicle platooning subject to uncertain disturbances via super-twisting second-order sliding-mode observer technique," *IEEE Transactions on Vehicular Technology*, vol. 71, no. 7, pp. 7186–7201, 2022.

[4] P. Fernandes and U. Nunes, "Multiplatooning leaders positioning and cooperative behavior algorithms of communicant automated vehicles for high traffic capacity," *IEEE Transactions on Intelligent Transportation Systems*, vol. 16, no. 3, pp. 1172–1187, 2015.

[5] X. T. Yang, K. Huang, Z. Zhang, Z. A. Zhang, and F. Lin, "Eco-driving system for connected automated vehicles: Multi-objective trajectory optimization," *IEEE Transactions on Intelligent Transportation Systems*, vol. 22, no. 12, pp. 7837–7849, 2021.

[6] Y. Bian, C. Du, M. Hu, S. E. Li, H. Liu, and C. Li, "Fuel economy optimization for platooning vehicle swarms via distributed economic model predictive control," *IEEE Transactions on Automation Science and Engineering*, vol. 19, no. 4, pp. 2711–2723, 2022.

[7] D. Chen, S. Ahn, M. Chitturi, and D. A. Noyce, "Towards vehicle automation: Roadway capacity formulation for traffic mixed with regular and automated vehicles," *Transportation research part B: methodological*, vol. 100, pp. 196–221, 2017.

[8] C. Zhai, F. Luo, Y. Liu, and Z. Chen, "Ecological cooperative look-ahead control for automated vehicles travelling on freeways with varying slopes," *IEEE Transactions on Vehicular Technology*, vol. 68, no. 2, pp. 1208–1221, 2019.

[9] M. Hu, C. Li, Y. Bian, H. Zhang, Z. Qin, and B. Xu, "Fuel economy-oriented vehicle platoon control using economic model predictive control," *IEEE Transactions on Intelligent Transportation Systems*, vol. 23, no. 11, pp. 20 836–20 849, 2022.

[10] A. Alam, B. Besselink, V. Turri, J. MåRtensson, and K. H. Johansson, "Heavy-duty vehicle platooning for sustainable freight transportation: A cooperative method to enhance safety and efficiency," *IEEE Control Systems Magazine*, vol. 35, no. 6, pp. 34–56, 2015.

[11] F. Browand and M. Hammache, "The limits of drag behavior for two bluff bodies in tandem," 2004. [Online]. Available: https://api.semanticscholar.org/CorpusID:110981612

[12] P. Zhang, D. Tian, J. Zhou, X. Duan, Z. Sheng, D. Zhao, and D. Cao, "Joint optimization of platoon control and resource scheduling in cooperative vehicle-infrastructure system," *IEEE Transactions on Intelligent Vehicles*, vol. 8, no. 6, pp. 3629–3646, 2023.

[13] D. Jia, K. Lu, J. Wang, X. Zhang, and X. Shen, "A survey on platoon-based vehicular cyber-physical systems," *IEEE Communications Surveys & Tutorials*, vol. 18, no. 1, pp. 263–284, 2016.

[14] X. Hu, L. Xie, L. Xie, S. Lu, W. Xu, and H. Su, "Distributed model predictive control for vehicle platoon with mixed disturbances and model uncertainties," *IEEE Transactions on Intelligent Transportation Systems*, vol. 23, no. 10, pp. 17 354–17 365, 2022.

[15] X. Sun and Y. Yin, "Behaviorally stable vehicle platooning for energy savings," *Transportation Research Part C: Emerging Technologies*, vol. 99, pp. 37–52, 2019.

[16] U. Ojha and M.-Y. Chow, "Behavioral control based adaptive bandwidth allocation in a system of unmanned ground vehicles," in *IECON 2010-36th Annual Conference on IEEE Industrial Electronics Society*. IEEE, 2010, pp. 3123–3128.

[17] J. Zeng, Y. Qian, J. Li, Y. Zhang, and D. Xu, "Congestion and energy consumption of heterogeneous traffic flow mixed with intelligent connected vehicles and platoons," *Physica A: Statistical Mechanics and its Applications*, vol. 609, p. 128331, 2023.

[18] T. T. Phan, D. Ngoduy, and L. B. Le, "Space distribution method for autonomous vehicles at a signalized multi-lane intersection," *IEEE Transactions on Intelligent Transportation Systems*, vol. 21, no. 12, pp. 5283–5294, 2019.

[19] S. Baldi, D. Liu, V. Jain, and W. Yu, "Establishing platoons of bidirectional cooperative vehicles with engine limits and uncertain dynamics," *IEEE Transactions on Intelligent Transportation Systems*, vol. 22, no. 5, pp. 2679–2691, 2021.

[20] M. Farina, L. Giulioni, L. Magni, and R. Scattolini, "An approach to output-feedback mpc of stochastic linear discrete-time systems," *Automatica*, vol. 55, pp. 140–149, 2015.

[21] J. Lan and D. Zhao, "Min-max model predictive vehicle platooning with communication delay," *IEEE Transactions on Vehicular Technology*, vol. 69, no. 11, pp. 12 570–12 584, 2020.

[22] S. Woo and A. Skabardonis, "Flow-aware platoon formation of connected automated vehicles in a mixed traffic with human-driven vehicles," *Transportation research part C: emerging technologies*, vol. 133, p. 103442, 2021.

[23] M. Hammache, M. Michaelian, and F. Browand, "Aerodynamic forces on truck models, including two trucks in tandem," 03 2002.

[24] M. Xu, Y. Luo, W. Kong, and K. Li, "A distributed model predictive control method combined with delay compensator for multiple vehicle platoons," *IET Intelligent Transport Systems*, vol. 17, no. 2, pp. 357–372, 2023.

[25] A. Roshko and K. Koenig, *Interaction Effects on the Drag of Bluff Bodies in Tandem*. Boston, MA: Springer US, 1978, pp. 253–286.

[26] S. Tsugawa, S. Jeschke, and S. E. Shladover, "A review of truck platooning projects for energy savings," *IEEE Transactions on Intelligent Vehicles*, vol. 1, no. 1, pp. 68–77, 2016.

[27] X. Sun and Y. Yin, "Decentralized game-theoretical approaches for behaviorally-stable and efficient vehicle platooning," *Transportation Research Part B: Methodological*, vol. 153, pp. 45–69, 2021.

[28] "The optimal eco-friendly platoon formation strategy for a heterogeneous fleet of vehicles," *Transportation Research Part D: Transport and Environment*, vol. 90, p. 102664, 2021.

[29] H. Liu, X. Kan, S. E. Shladover, X.-Y. Lu, and R. E. Ferlis, "Impact of cooperative adaptive cruise control on multilane freeway merge capacity," *Journal of Intelligent Transportation Systems*, vol. 22, no. 3, pp. 263–275, 2018.

[30] J. Wang, X. Luo, J. Yan, and X. Guan, "Distributed integrated sliding mode control for vehicle platoons based on disturbance observer and multi power reaching law," *IEEE Transactions on Intelligent Transportation Systems*, vol. 23, no. 4, pp. 3366–3376, 2022.

[31] Q. Luo, A.-T. Nguyen, J. Fleming, and H. Zhang, "Unknown input observer based approach for distributed tube-based model predictive control of heterogeneous vehicle platoons," *IEEE Transactions on Vehicular Technology*, vol. 70, no. 4, pp. 2930–2944, 2021.

[32] Z. Ju, H. Zhang, and Y. Tan, "Distributed stochastic model predictive control for heterogeneous vehicle platoons subject to modeling uncertainties," *IEEE Intelligent Transportation Systems Magazine*, vol. 14, no. 2, pp. 25–40, 2022.

[33] J. Zhou, D. Tian, Z. Sheng, X. Duan, G. Qu, D. Zhao, D. Cao, and X. Shen, "Robust min-max model predictive vehicle platooning with causal disturbance feedback," *IEEE Transactions on Intelligent Transportation Systems*, vol. 23, no. 9, pp. 15 878–15 897, 2022.

[34] D. Mayne, M. Seron, and S. Raković, "Robust model predictive control of constrained linear systems with bounded disturbances," *Automatica*, vol. 41, no. 2, pp. 219–224, 2005.

[35] "Robust distributed model predictive platooning control for heterogeneous autonomous surface vehicles," *Control Engineering Practice*, vol. 107, p. 104655, 2021.

[36] H. Zeng, Z. Ye, and D. Zhang, "Robust model predictive control based cooperative control of uncertain connected vehicle platoon systems," in *2023 9th International Conference on Control, Automation and Robotics (ICCAR)*, 2023, pp. 256–261.

[37] Y. Liu, C. Zong, C. Dai, H. Zheng, and D. Zhang, "Behavioral decision-making approach for vehicle platoon control: Two noncooperative game models," *IEEE Transactions on Transportation Electrification*, vol. 9, no. 3, pp. 4626–4638, 2023.

[38] X. Cheng, Q. Yao, M. Wen, C.-X. Wang, L.-Y. Song, and B.-L. Jiao, "Wideband channel modeling and intercarrier interference cancellation for vehicle-to-vehicle communication systems," *IEEE Journal on Selected Areas in Communications*, vol. 31, no. 9, pp. 434–448, 2013.

[39] T. Jiang, H.-H. Chen, H.-C. Wu, and Y. Yi, "Channel modeling and inter-carrier interference analysis for v2v communication systems in frequency-dispersive channels," *Mobile Networks and Applications*, vol. 15, pp. 4–12, 2010.

[40] V. G. Stepanyants and A. Y. Romanov, "A survey of integrated simulation environments for connected automated vehicles: Requirements, tools, and architecture," *IEEE Intelligent Transportation Systems Magazine*, 2023.

[41] M. M. Şahin, O. Dizdar, B. Clerckx, and H. Arslan, "Ofdm-rsma: Robust transmission under inter-carrier interference," *IEEE Transactions on Communications*, 2024.

[42] G. Scora and M. Barth, "Comprehensive modal emissions model (cmem), version 3.01," *User guide. Centre for environmental research and technology. University of California, Riverside*, vol. 1070, p. 1580, 2006.

[43] D. C. Quiros, J. Smith, A. Thiruvengadam, T. Huai, and S. Hu, "Greenhouse gas emissions from heavy-duty natural gas, hybrid, and conventional diesel on-road trucks during freight transport," *Atmospheric Environment*, vol. 168, pp. 36–45, 2017.

[44] S. Gong, J. Shen, and L. Du, "Constrained optimization and distributed computation based car following control of a connected and autonomous vehicle platoon," *Transportation Research Part B: Methodological*, vol. 94, pp. 314–334, 2016.

[45] D. Liu, S. Baldi, and S. Hirche, "Collision avoidance in longitudinal platooning: Graceful degradation and adaptive designs," *IEEE Control Systems Letters*, vol. 7, pp. 1694–1699, 2023.

[46] P. Zhang, Y. Liu, G. Yang, and G. Zhang, "A distributionally robust optimization model for designing humanitarian relief network with resource reallocation," *Soft Computing*, vol. 24, pp. 2749–2767, 2019.

[47] A. Ben-Tal, L. El Ghaoui, and A. Nemirovski, *Robust optimization*. Princeton university press, 2009, vol. 28.

[48] S. Boyd, S. P. Boyd, and L. Vandenberghe, *Convex optimization*. Cambridge university press, 2004.

[49] C. PeMS, "Caltrans performance measurement system (pems)," *US DOT*, 2021.

[50] J. Yang, D. Zhao, J. Lan, S. Xue, W. Zhao, D. Tian, Q. Zhou, and K. Song, "Eco-driving of general mixed platoons with cavs and hdvs," *IEEE Transactions on Intelligent Vehicles*, vol. 8, no. 2, pp. 1190–1203, 2022.

[51] D. Swaroop and J. Hedrick, "String stability of interconnected systems," in *Proceedings of 1995 American Control Conference-ACC'95*, vol. 3, 1995, pp. 1806–1810 vol.3.

Peiyu Zhang received her M.Sc. degree in mathematics from Hebei University, Baoding, China, in 2020, and the Ph.D. degrees in traffic information engineering and control from Beihang University, Beijing, China in 2024. She is currently a Post-Doctoral Research Fellow with Beijing Institute of Technology. Her main research interests include vehicle platoon control, intelligent transportation systems and robust optimization.

Daxin Tian received his Ph.D degree in computer application technology from Jilin University, Changchun, China, in 2007. He is currently a professor with the School of Transportation Science and Engineering, Beihang University, Beijing, China. His research is focused on intelligent transportation systems, autonomous connected vehicles, swarm intelligent and mobile computing. He was awarded the Changjiang Scholars Program (Young Scholar) of Ministry of Education of China in 2017, the National Science Fund for Distinguished Young Scholars in 2018, and the Distinguished Young Investigator of China Frontiers of Engineering in 2018. He is also a sensor member of the IEEE ans served as the Technical Program Committee member/Chair/Co-Chair for several international conferences including EAI 2018, ICTIS 2019, IEEE ICUS 2019, IEEE HMWC 2020, GRAPH-HOC 2020, etc.

Jianshan Zhou received the B.Sc., M.Sc., and Ph.D. degrees in traffic information engineering and control from Beihang University, Beijing, China, in 2013, 2016, and 2020, respectively. He is an associate professor with the school of transportation science and engineering at Beihang University. From 2017 to 2018, he was a Visiting Research Fellow with the School of Informatics and Engineering, University of Sussex, Brighton, U.K. He was a Postdoctoral Research Fellow supported by the Zhuoyue Program of Beihang University and the National Postdoctoral Program for Innovative Talents from 2020 to 2022. He is or was the Technical Program Session Chair with the IEEE EDGE 2020, the IEEE ICUS 2022, the ICAUS 2022, the TPC member with the IEEE VTC2021-Fall track, and the Youth Editorial Board Member of the Unmanned Systems Technology. He is the author or co-author of more than 30 international scientific publications. His research interests include the modeling and optimization of vehicular communication networks and air–ground cooperative networks, the analysis and control of connected autonomous vehicles, and intelligent transportation systems. He was the recipient of the First Prize in the Science and Technology Award from the China Intelligent Transportation Systems Association in 2017, the First Prize in the Innovation and Development Award from the China Association of Productivity Promotion Centers in 2020, the Second Prize in the Beijing Science and Technology Progress Award in 2022, the National Scholarships in 2017 and 2019, the Outstanding Top-Ten Ph.D. Candidate Prize from Beihang University in 2018, the Outstanding China-SAE Doctoral Dissertation Award in 2020, and the Excellent Doctoral Dissertation Award from Beihang University in 2021.

Xuting Duan received the Ph.D. degree in traffic information engineering and control from Beihang University, Beijing, China. He is currently a Professor with the School of Transportation Science and Engineering, Beihang University. His research interests are focused on the theories of V2X communications and collaborative intelligence, as well as their systematic engineering applications in three-dimensional intelligent transportation systems, connected and autonomous vehicles, and cross-domain collaborative unmanned systems.

Dezong Zhao received the B.Eng. and M.S. degrees from Shandong University, Jinan, China, in 2003 and 2006, respectively, and the Ph.D. degree from Tsinghua University, Beijing, China, in 2010, all in Control Science and Engineering. He is a Senior Lecturer in Autonomous Systems with the School of Engineering, University of Glasgow, U.K. Dr Zhao's research interests include connected and autonomous vehicles, machine learning and control engineering. His work has been recognised by being awarded an EPSRC Innovation Fellowship and a Royal Society-Newton Advanced Fellowship in 2018 and 2020, respectively.

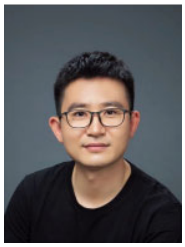

Dongpu Cao received the Ph.D. degree from Concordia University, Canada, in 2008. He is the Canada Research Chair in Driver Cognition and Automated Driving, and currently an Associate Professor and Director of Waterloo Cognitive Autonomous Driving (CogDrive) Lab at University of Waterloo, Canada. His current research focuses on driver cognition, automated driving and cognitive autonomous driving. He has contributed more than 200 papers and 3 books. He received the SAE Arch T. Colwell Merit Award in 2012, IEEE VTS 2020 Best Vehicular Electronics Paper Award and three Best Paper Awards from the ASME and IEEE conferences. Prof. Cao serves as Deputy Editor-in-Chief for IET INTELLIGENT TRANSPORT SYSTEMS JOURNAL, and an Associate Editor for IEEE Transactions on Vehicular Technology, IEEE Transactions on intelligent transportation systems, IEEE/ASME Transactions on Mechatronics, IEEE Transactions on Industrial Electronics, IEEE/CAA JOURNAL OF AUTOMATICA SINICA, IEEE Transactions on computational social systems, and ASME Journal of Dynamic Systems, Measurement and Control. He was a Guest Editor for Vehicle System Dynamics, IEEE TRANSACTIONS ON SMC: SYSTEMS and IEEE INTERNET OF THINGS JOURNAL. He serves on the SAE Vehicle Dynamics Standards Committee and acts as the Co-Chair of IEEE ITSS Technical Committee on Cooperative Driving.

Luzheng Bi received the Ph. D. degree in mechanical engineering from the Beijing Institute of Technology, Beijing, China, in 2004. From 2007 to 2008, he was a visiting scholar with the Department of Industrial and Operations Engineering, University of Michigan, Ann Arbor. From Nov. 2017 to May 2018, he was a visiting scholar with the Department of Computer Science and Engineering, Nanyang Technological University, Singapore. He is currently a Professor and the Director of the Institute of Mechatronic Systems, Beijing Institute of Technology. His research interests include intelligent systems, brain-controlled robots and vehicles, human-machine collaboration, and human behavior modeling. Prof. Bi is Associate Editors of Complex System Modeling and Simulation, IEEE/ASME AIM, ASME DSCC, ACC, and CCC. He is an author of refereed journal articles in the IEEE Transactions on Cybernetics, IEEE Transactions on Intelligent Transportation Systems, IEEE Transactions on Biomedical Engineering, IEEE Transactions on Neural Systems and Rehabilitation Engineering, IEEE Transactions on System, Man, and Cybernetics, and other journals. Prof. Bi received the Natural Science Award by the Ministry of Education of China and Electronics and Information Science and Technology Award by the Chinese Society of Electronics. He was the recipient of the Supervisor Awards of Outstanding Doctoral Dissertation and of Outstanding Master Thesis of the Beijing Institute of Technology.